Tension change of *Xenopus laevis* oocytes influences Rho GTPase regulation of wound healing

Tatsuya Kato

Department of Anatomy and Cell Biology

McGill University, Montreal

May 2018

A thesis submitted to McGill University in partial fulfillment of the requirements of the degree of Master of Science in Anatomy and Cell Biology

I. Table of Contents

II. Table of Figures

III. Table of Tables

IV. Abstract

Introduction: Living cells need to respond to a myriad of mechanical forces for their continued survival and function. This is rendered possible by the cell's ability to maintain homeostasis of its own structural and tensile stability, referred to as tensegrity. When a cell is wounded, this homeostasis is compromised in the form of transient tension increase at the wound site. To restore cellular tensegrity after wounding, cells must repair the damage done to its plasma membrane and cytoskeleton. Cytoskeletal repair through its reorganization is controlled by activities of Rho GTPases RhoA and Cdc42 which regulate the formation and contraction of an actomyosin ring around the wound. Recruitment of these Rho GTPases are recognized to depend on Ca^{2+} influx and the dynamic changes in plasma membrane lipid domains that occurs upon wounding. However, the effect of the changes in cell-wide and local tension arising from the wound damage on the regulation of actomyosin-mediated wound healing has yet to be thoroughly explored.

Hypothesis: Transient local tension increase is necessary for actomyosin-mediated wound healing.

Methods: To decrease wound-induced tension dynamics at the local wound site, *Xenopus laevis* oocytes were incubated in hyperosmotic sucrose media of various concentrations. This cell tension decrease was confirmed through comparative measurements of oocyte Young's moduli via microindentation. Cell tension reduction's influence on actomyosin ring regulation was then observed by time lapse confocal microscopy. RhoA and Cdc42 activity levels were also analyzed in western blot and pulldown assays.

Results: Dose-dependent decrease in Young's moduli was confirmed in sucrose media-incubated oocytes. Sucrose-treated oocytes were observed to heal wounds more slowly, with decreased wound peripheral enrichment of actin and active RhoA. In contrast, active Cdc42 accumulation around the wound was unchanged. At the cell-wide level, decreased levels of active RhoA and increased levels of active Cdc42 were observed in sucrose-treated oocytes.

Conclusions: The cell's Rho GTPase regulation of its actomyosin-mediated wound healing response requires transient cell tension increase at the local wound site.

V. Résumé

Introduction: Afin d'assurer leur survie, les cellules doivent être capables de s'adapter à une myriade de forces mécaniques. Elles y arrivent en maintenant les forces les affectants dans un état d'homéostasie dynamique leur conférant un certain degré de stabilité structurelle et est souvent décrite sous l'égide du mot-valise tenségrité. Lorsque qu'une cellule est endommagée, sa tenségrité est interrompue, menant à une augmentation transitoire de la tension autours du dommage cellulaire. La cellule endommagée se doit donc de réparer les dommages faits à sa membrane plasmidique et à son cytosquelette. La réparation du cytosquelette est orchestrée par l'activité coordonné de RhoA et de Cdc42 qui régule la formation et la contraction d'un anneau d'actomyosine se formant autour de la "plaie" cellulaire. La formation de cet anneau est reconnu de dépendre principalement del'influx de calcium et les changements de composition lipidique de la membrane plasmidique qui accompagnent les dommages cellulaires. En revanche, la présence d'une possible relation entre les changements dynamiques de tension ayant lieux au site de dommages cellulaires et la réparation cellulaire médiée par la formation et la contraction d'un anneau d'actomyosine reste entièrement inexplorée.

Hypothèse: L'augmentation de la tension locale transitoire aux sites de dommage cellulaire est nécessaire pour la réparation cellulaire médiée par la formation et la contraction d'anneau actomyosine.

Méthodes: Afin de diminuer les changements dynamiques de tension ayant lieux au site de dommages cellulaires, des ovocytes de *Xenopus laevis* furent incubés dans des milieux de cultures hypertoniques. L'efficacité de ces traitements fut ensuite confirmée en mesurant le module d'élasticité (module de Young) des ovocytes traités et d'ovocytes contrôles par microindentation. L'impact de la diminution de la tension sur la réparation cellulaire et la formation d'anneaux d'actomyosine fut ensuite directement évaluée par microscopie confocale. Les niveaux de RhoA, de Cdc42 furent également évalués par le biais d'immunotransferts (western blots) et d'immunoprécipitations.

Résultats: Tel qu'attendu, les ovocytes incubés dans les milieux hypertoniques avaient des modules d'élasticités nettement plus bas que les ovocytes contrôles, ce qui serait compatible avec une diminution de la tension cellulaire dans ces ovocytes. Parallèlement, les ovocytes incubés dans

les milieux hypertoniques montraient de sévères lacunes en ce qui concerne la réparation du cytosquelette et avaient des diminutions notables dans l'enrichissement d'actine et de RhoA actif en périphérie des plaies cellulaires. En revanche, l'accumulation de Cdc42 actif autour de la plaie était inchangée. Nos résultats d'immunotransferts et d'immunoprécipitations ont également révélés la présence de niveaux réduits de RhoA actif et des niveaux accrus de Cdc42 actif dans les extraits d'ovocytes incubés dans les milieux hypertoniques.

Conclusions: La présence d'une augmentation transitoire de tension locale aux sites de dommage cellulaire est nécessaire pour la réparation cellulaire médiée par la formation et la contraction d'anneau d'actomyosine.

VI. Acknowledgements

Firstly, I thank Dr. Craig Mandato for giving me the opportunity to work in his laboratory as a graduate student and supervising the project. I thank Dr. Eric Boucher for his contribution to the study design, invaluable assistance in all experiments and techniques, and French translation of the study abstract. I thank Peter Holder for helping prepare samples.

I also thank Dr. Allen Erhlicher for his advice as well as granting me access to his laboratory and equipment. I thank Dr. Hossein Khadivi Heris for much of the coding in the MATLAB program used to control the microindenter and help in microindenter calibration. I thank Tao Jiang for his help in additional MATLAB coding.

I further thank department faculty members Dr. Chantelle Autexier, Dr. Susanne Bechstedt, Dr. Khanh Huy Bui, and Dr. Dieter Reinhardt for their constructive feedback and attendance in my academic presentations.

I thank all the department administrators for their help. In particular, I thank Joseph Dube for his counseling support.

I thank Corina DeKraker, Angela Dong, Logine Ghadban, Gary Wang, and David Zhou for their help and support as fellow lab members.

Finally, I thank my family and friends for their continuous encouragement and support throughout this period of study.

VII. Contribution of Authors

Tatsuya Kato wrote all chapters of the manuscript in consultation with Dr. Craig Mandato and Dr. Eric Boucher. The abstract was translated into French by Dr. Eric Boucher.

Chapter 1:
Introduction

1. Introduction

1.1. Literature review

1.1.1. The single cell as a tensegrity model

Living cells possess the innate ability to respond and adapt to a myriad of mechanical forces to continually survive and perform their functions. Such an ability is biophysically founded on the cell's dynamic maintenance of its structural integrity, which in turn depends on a stabilized equilibrium of continuous apparent membrane tension. Cell-wide tensile prestress primarily consists of the spatiotemporal organization of counterbalancing intracellular forces from tension-generating and compression-resisting cytoskeletal elements (see Section 1.1.2). This intracellular structural organization is the foremost principle of cellular tensegrity (reviewed in [1]), the mechanobiological application of tensegrity (tensile-integrity) structures which were first proposed by architect and systems theorist Buckminster Fuller [2].

Application of the cellular tensegrity model has proven particularly useful to study cell morphogenic changes in both structural and mechanical contexts. The tensegrity model has been utilized to elucidate formations of molecular self-assemblies such as cytoskeletal geodomes [3-5], polyhedral enzyme complexes [6] and clathrin-coated vesicles [7], all structurally akin to the Montreal Biosphere designed by Fuller. The model also provided an initial consensus for various plasma membrane forces, measured using a similar variety of cell models and experimental methods which were previously confusing and less intuitive to link together (reviewed in [8, 9]). In contrast to previous conclusions of being cell type or method specific, the tensegrity model-derived interpretation of these forces as decoupled components of equilibrium apparent membrane tension has advanced understanding of each component force (Table 1), as well as robust quantifications of total cell elasticities [10]. Further biomechanical understanding has also led to

complications in cell modeling and measuring, such as the difficulties in recapitulating nonlinear viscoelasticity of cytoskeletal networks [11, 12] and dynamic force contributions from crosslinkers [13, 14]. Though these challenges have uncovered technical limitations of the basic "cable-strut" cellular tensegrity model (reviewed in [15]), it remains fundamentally powerful when its concept is applied to processes of single cell cytoskeletal dynamics. Since apparent membrane tension represents total tension present in the plasma membrane which defines cell boundaries, apparent membrane tension and cell tension will be interchangeably used.

Table 1. Component forces of apparent membrane tension in the cell.

Component	Other names	Definition	Origin	Models / Method(s)
Membrane components				
Plasma membrane tension	-	Tension of the plasma membrane proper	Hydrostatic pressure difference between cytosol and extracellular fluid [16]	Human melanoma cell lines [17] / Micropipet aspiration [17, 18]
Membrane bending stiffness	Curvature elastic modulus [19], bending resistance [20]	Resistance of phospholipid bilayer to radial elastic deformations [21]	Stress resultant difference between phospholipid monolayers [20]	Erythrocytes [22], liposomes [19, 23] / Micropipet aspiration [19], shape fluctuation spectroscopy [24]
Line tension	Edge energy [25], lipid disorder [26]	Tension produced from disordered arrangements of membrane phospholipids [25]	Chemical potential difference between phospholipids of the wound edge and planar membrane [27]	Giant lecithin vesicles [25], giant unilamellar vesicles [28], liposomes [27] / Mathematical models [25, 27-29]
Cytoskeletal components				
MCA[1] force	Membrane-cytoskeleton adhesion, tether force	Force of adhesion between plasma membrane and cytoskeleton [30]	Plasma membrane-cytoskeleton interactions via cortical actin, transmembrane proteins, etc.	BAECs[2] [31], neuronal growth cones [32], HEK293[3] cells [31], MEFs[4] [31] / AFM[5], FRET[6], optical tweezers [31]

[1]Membrane-to-cortex attachments; [2]Bovine aortic endothelial cells; [3]Human embryonic kidney 293; [4]Mouse embryonic fibroblasts; [5]Atomic force microscopy; [6]Fluorescence resonance energy transfer

1.1.2. Cytoskeleton: Primary stabilizer of cell structural integrity

As a tensegrity system the cell heavily depends on its cytoskeleton, a complex network of interlinked filaments and tubules, for structural maintenance. Much of this network is comprised by two highly conserved protein polymers, actin filaments and microtubules, which reciprocally generate tension and resist compression. The third polymer class of intermediate filaments, and a host of accessory proteins, complete as well as enhance cytoskeletal structure and function.

The tension-generating filamentous actin (F-actin) is the polymerized form of globular actin (G-actin) monomers which self-assemble into ~8nm-wide double helix filaments (Figure 1A, red). F-actin meshworks are highly concentrated at the cell cortex immediately beneath the plasma membrane, generating contractile forces [33] that constitute most of the membrane-to-cortex attachments (MCA) component of apparent membrane tension (Table 1). Numerous associated proteins actuate MCA force generation, such as myosin filaments (Figure 1A, purple) which exert additional Ca^{2+}-dependent contractile forces (see Section 1.1.5.1), crosslinkers like α-actinin and filamin which mediate F-actin crosslinking [34, 35], as well as the ezrin, radixin, moesin (ERM) proteins [36] and transmembrane proteins which link F-actin with the plasma membrane (reviewed in [37, 38]). The integrated contractile activity of the actin-myosin complex (actomyosin) is especially central to overall cytoskeletal structure and function, hence will be referred to repeatedly.

Compression-resisting microtubules result from cylindrical polymerization of αβ-tubulin dimers into tubules with ~25nm, 13-dimer diameters (Figure 1A, green). This hollow tubular structure confers high bending rigidity which primarily enables compression resistance [39]. Like those of actin, there are a variety of proteins that interact with microtubules which augment its structural function and grant it additional ones. Microtubule-associated proteins (MAPs) such as MAP1/2/4

and tau directly crosslink microtubules with F-actin (reviewed in [40]), which dramatically increase compressive forces that microtubules can sustain [41], as well as allow them to influence actomyosin activities (see Section 1.1.3.2). Furthermore, motor proteins namely kinesins and dyneins shuttle molecular cargo along microtubules in anterograde and retrograde directions respectively, bestowing microtubules with their other important function as "cellular highways."

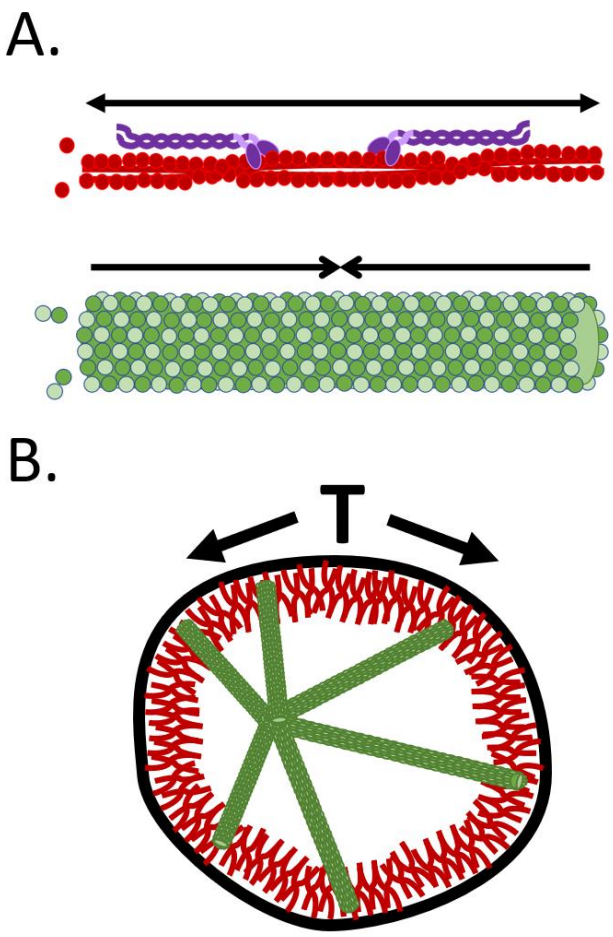

Figure 1. Tensile and compressive elements of the single cell tensegrity model.

(A) Actin (red circles) and myosin (in purple) filaments generate much of the tensile forces (closed arrow) in a cell, while microtubules (dark and light green circles) resist the reciprocal compressive forces (open arrow). **(B)** Organized arrangements of cortical actin filaments (red) and microtubules (green) are primarily responsible for the cell's maintenance of its apparent membrane tension, *T*.

The third major cytoskeletal components of intermediate filaments (IFs) additionally support tertiary cellular structure. IF subunits aggregate into flexible ropelike tetramer assemblies with ~10nm widths. Unlike actin and tubulin monomers, IF subunits constitute a large heterogenous family which leads to versatile IF localizations varying across cell types. Though not as structurally conserved as its cytoskeletal counterparts, IFs such as vimentin have been observed to also contribute to cell structure maintenance through tension generation [42, 43]. Furthermore, considering IF's formation into nuclear lamina underlying the nuclear envelope (reviewed in [44]), investigations specific for IF structure are of potential interest when integrating nuclear membrane as the inner component of a hierarchical cellular tensegrity system (reviewed in [45]), though this avenue of cytoskeletal structure is not explored in this thesis.

The above cytoskeletal components, arranged with their many associated proteins, stabilize the equilibrium of apparent membrane tension (Figure 1B). In addition, the polymeric nature and associated protein interactions particularly enable F-actin and microtubules to also rapidly grow or shrink depending on multiple extracellular mechanical and intracellular biochemical cues (see Sections 1.1.3.2, 1.1.5.1 and 1.1.6). Cytoskeletal dynamics enable cells to quickly respond to disruptive mechanical forces while minimizing compromise of structural integrity.

At the basic biochemical level, cytoskeletal dynamics are characterized by indefinite phases of F-actin and microtubule growth fluctuations. Each G-actin monomer carries a tightly-bound ATP molecule as they aggregate into F-actin. Similarly, αβ-tubulin dimers are bound to two GTP molecules in the case of microtubule assembly. Shortly after incorporation, hydrolysis activities of G-actin [46] and β-tubulin (the α-tubulin-GTP bond being more stable) [47] cause conformation changes and reduce binding affinity to its neighboring subunits [48, 49], increasing the probability of polymer dissociation. This dissociative propensity of ADP/GDP-bound subunits imparts critical

dependence of polymer length stability on an equilibrium concentration of free monomers named the critical concentration (C_c), above and below which polymers dynamically grow and shrink [50, 51]. Meanwhile, conformation differences between ATP/GTP-bound and ADP/GDP-bound subunits lead to different C_c at each polymer end, causing faster and slower assembly rates which results in asymmetric polymerization at the plus and minus ends respectively. This polarity further results in directed motility with a C_c-dependent steady state called treadmilling, in which subunits newly assembled at the plus end travel on the polymer as if on a treadmill until dissociating at the minus end [52]. In this way, the destabilizing effect of nucleotide hydrolysis confer both transience and variable directionality to polymerizations of F-actin and microtubules.

The above cytoskeletal fluxes are represented as cortical flow of F-actin and dynamic instability of microtubules in the larger context of cellular processes. Due to the unstable nature of individual hydrolyzed subunits, polymers minimally require nucleus formations of G-actin trimers, or rings of 13 αβ-tubulin dimers, to stably grow in length. To expedite this rate-limiting nucleation process, cells synthesize protein complexes specialized in assembly initiation, such as the actin-related protein 2/3 (Arp2/3) complex [53] and the γ-tubulin ring complex (γ-TuRC) [54]. Other associated proteins, such as profilin [55] and cofilin [56] which promote and inhibit F-actin nucleation respectively, as well as XMAP215 [57] and TPX2 [58] which stimulate tubule nucleation, further enhance cytoskeletal dynamics. Coordinations of F-actin and microtubule treadmilling activities with associated proteins, as well as with each other, are the structural basis of morphogenic changes cells perform in response to mechanical cues (reviewed in [59]), such as cellular wound healing [60] (see Section 1.1.3.2), migration [61] and division [62].

1.1.3. Single-cell healing of mechanical wounds

Cell wounding results from many avenues of threats, and there are wound types not of purely physical origin such as those induced by pore-forming proteins or toxins (reviewed in [63]). This thesis focuses on mechanical wounds, which are characterized by direct physical disruptions of the cell's plasma membrane and underlying cytoskeleton. A variety of healing mechanisms in quick response to mechanical wounds have been observed in a similar range of cell types. Therefore it is unsurprising that numerous intrinsic and extrinsic factors appear to influence the repair mechanism deployed, including cell size, cell shape, plasma membrane composition, intracellular proteins, local microenvironment, extracellular ions, and wound size (reviewed in [64]). That said, almost all wound healing processes follow the two generally conserved phases of plasma membrane resealing and cytoskeletal reorganization. Later sections focus on aspects of cytoskeletal reorganization observed in *Xenopus laevis* oocytes responding to large (>1μm) mechanical wounds.

1.1.3.1. *Plasma membrane resealing: "Membrane patch"*

Upon wound-induced plasma membrane disruption and failure of membrane barrier function (Figure 2A), immediate Ca^{2+} influx promotes homotypic fusions of intracellular vesicles [65]. Rapid accumulation of such Ca^{2+}-dependent fusogenic events results in formation of a large "membrane patch" vesicle which spans the wound [66] and temporarily prevents cell lysis through further ion influx and cellular damage [67] (Figure 2B). More recent iterations of this membrane patching hypothesis have additionally incorporated subsequent processes of membrane continuity restoration which ultimately ensure more permanent resealing. An example is the mediation of "vertex fusion," which consists of homotypic fusions at circumferential vertices periphery to the

wound, and exocytic shedding of the membrane patch remnant (reviewed in [68]). First observed during homotypic fusions of yeast vacuoles [69, 70], this process has yet to be confirmed in other cell models. Another possibility is that of the actomyosin intermediate, in which further fusions of intracellular vesicles, membrane patch and wound edges restore membrane composition and continuity, while simultaneous actomyosin contraction structurally reinforces the repairing membrane borders and restores overall cortex morphology (Figure 3; see Section 1.1.3.2). However, such contractile activity is not necessarily mutually exclusive from "vertex fusion" and patch shedding in the context of membrane continuity restoration. Although initial post-wound membrane dynamics consistent with membrane patching have since been directly visualized [71], the exact mechanisms of accompanying patch scission and/or contraction are still unresolved.

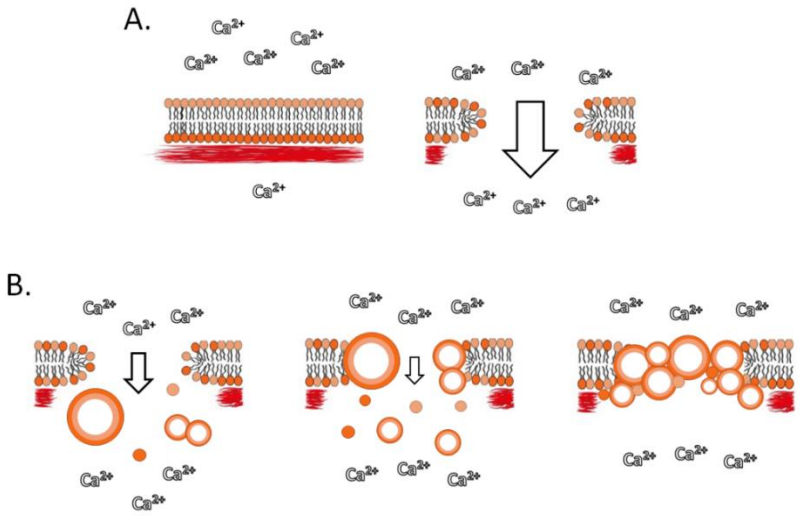

Figure 2. Membrane patch formation and sealing.

(A) The plasma membrane's barrier function is compromised upon its wounding, resulting in lipid disruption and influx of extracellular divalent cations (e.g. Ca^{2+}). **(B)** Membrane patching primarily consists of Ca^{2+}-dependent homotypic fusions of vesicles to the wound site, aggregation of which caps the plasma membrane, transiently preventing further cell damage and ion influx.

The “membrane patch” model of transient single-cell membrane repair heavily depends on rampant homotypic fusions [65]. Consequently, it has been particularly apparent in oocytes which are able to utilize yolk vesicles as readily available reserves [65, 66, 71, 72], with the latter’s storage of glycogen and lipid nutrients essential for embryonic development [73]. Mammalian somatic cells additionally utilize membrane proximal lysosomes [74, 75] to employ relatively nuanced heterotypic mechanisms of plasma membrane resealing. For example, it has been observed that large somatic cell membrane disruptions are distinctly removed through ceramide-mediated membrane invagination which relies on lysosomal acid sphingomyelinase (ASM) exocytosis (reviewed in [76]). To what extent these apparent differences are influenced by intrinsic oocyte biological properties (i.e. more readily available vesicles), or by biophysical factors of large wounds (i.e. faster Ca^{2+} influx rates), remains to be determined.

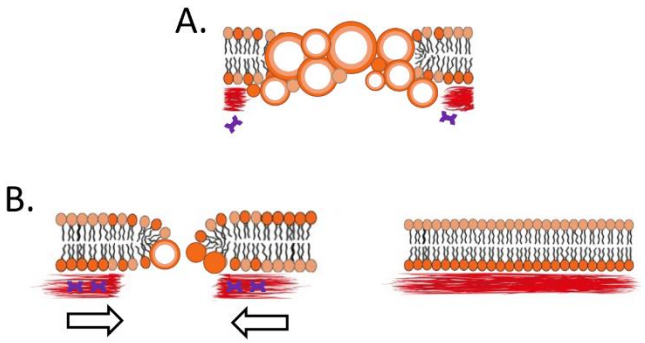

Figure 3. Reorganization and repair of cortical cytoskeleton.

(A) Following transient membrane patch formation, the underlying cortical cytoskeleton is still damaged and must be repaired to fully restore cell structural integrity. **(B)** To this end, the cytoskeleton is reorganized to close the wound, primarily through contraction powered by activities of actin (red) and myosin (purple). Within a few minutes the cortical cytoskeleton and adhered plasma membrane are repaired.

1.1.3.2. *Cytoskeletal reorganization: Actomyosin ring*

Just as the overall cytoskeleton maintains cellular tensegrity (see Section 1.1.2), the cortical cytoskeleton chiefly establishes membrane structural integrity. Thus, wound-induced cell cortex disruption significantly endangers cell shape maintenance and cell survival. In response, single cells reorganize and repair the cortical cytoskeleton through cytoskeletal dynamics, involving actomyosin contraction as well as translocations and *de novo* assemblies of F-actin and microtubules. These dynamics have been most extensively studied in the *Xenopus* model.

During the *Xenopus* oocyte's wound healing process, the newly formed wound-induced transient membrane patch (see Section 1.1.3.1) is encircled by an actomyosin ring, made from both local assembly of actin and myosin filaments at the wound edge, as well as wound-directed cortical flow of pre-existing F-actin [77] (Figure 3A). F-actin cortical flow during actomyosin array formation is mediated by a simultaneous locally assembled radial microtubule array, recruitment of which is reciprocally regulated by actomyosin contraction [60]. Feedback activities of cytoskeletal arrays lead to wound-directed contraction, and eventual constriction of the wound like a "purse string" [78] (Figures 3B, 4A). Further investigations of correlative changes in such actomyosin-microtubule spatiotemporal coordinations with those in localizations and activity levels of regulatory proteins have given profound insights into mechanisms of wound healing regulation at the molecular level.

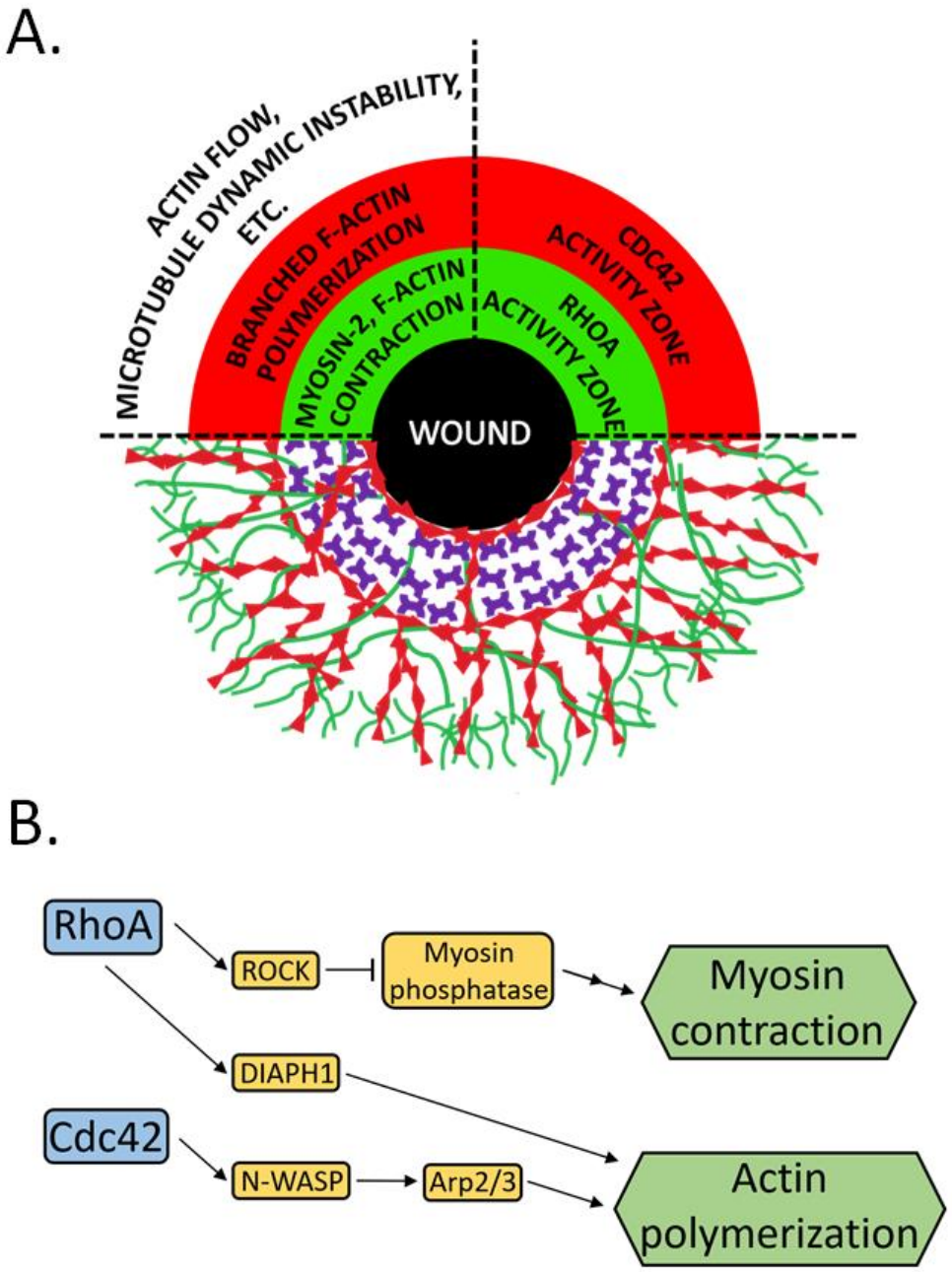

Figure 4. Activities of RhoA and Cdc42 regulate actomyosin-mediated wound healing.

(A) Overhead diagram of actomyosin contractile ring organization and regulation around the wound site. Top-left quadrant shows relevant cytoskeletal dynamics. Top-right quadrant shows concentric zones of Rho GTPase regulatory activities. Bottom half shows spatial organization of F-actin (red), myosin-2 (purple) and microtubules (green). **(B)** Signal transductions involved in actomyosin-mediated wound healing. Regulatory activities of RhoA and Cdc42 GTPases (blue) lead to modulations of their respective effector proteins (yellow), resulting in actomyosin activity (green).

Organized formation and contraction of the actomyosin ring are controlled by Rho family member A (RhoA) and cell division control protein 42 (Cdc42) Rho GTPases (Figure 4A; see Section 1.1.4). Within 30 seconds of cell wounding, their activities have been observed to be enriched in distinct and concentric zones around the wound, over time closing in concert with the contractile ring [79]. Active RhoA and Cdc42 trigger signal transductions in their zones which stimulate myosin contraction and actin polymerization (Figure 4B). RhoA activity encompasses immediately peripheral to the wound and regulates force generation necessary for ring contraction [79]. RhoA-induced activation of Rho-associated protein kinase (ROCK) [80] leads to inhibition of myosin phosphatase through myosin-binding subunit phosphorylation [81], which in turn negates the latter protein's inhibitory function on myosin light-chain kinase (MLCK). Active MLCK's phosphorylation of myosin-2's regulatory light chain then results in myosin-2 contraction which primarily drives ring closure. Active RhoA additionally interacts with diaphanous 1 (DIAPH1) formins [82], promoting polymerization of parallel actin filaments also responsible for contraction. Taken together, RhoA's dual modulation of ROCK and DIAPH1 enables coordinated actomyosin contraction [83, 84]. In the case of Cdc42, its activity encircles the inner RhoA zone to primarily regulate ring structure. Active Cdc42's interaction with neural Wiskott-Aldrich syndrome protein (N-WASP) [85] leads to the latter's activation, promoting C terminus binding with the Arp2/3 complex [86]. This stimulates the complex's actin nucleation activity resulting in polymerization of branched actin filaments with 70° angles [53]. Such radial arrangement of branched F-actin regulated in the active Cdc42 zone supports actomyosin ring structure throughout contraction [79].

1.1.4. Rho GTPases: Regulators of cytoskeletal dynamics

Since the initial discovery of the Ras proto-oncogene [87] the superfamily of over 150 rat sarcoma (Ras)-related small GTPases, and its functional classifications, have been identified [88]. One such subfamily, the Ras-homolog (Rho) GTPase family of cytoskeletal dynamics consists of 22 guanine nucleotide-binding hydrolases [89]. With continuing observations, such as that of rapid Swiss 3T3 fibroblast morphology and actin cytoskeleton changes upon recombinant Rho injection [90], these enzymes have become further illuminated as binary molecular switches of fundamental cytoskeletal reorganization processes common in all eukaryotic cells (reviewed in [91]), including wound repair. This thesis focuses on two specific Rho GTPases critical in this context, RhoA and Cdc42.

Rho GTPases' ability to function as molecular master switches for cytoskeletal dynamics is founded on three biochemical characteristics: bistability of activation states, plethora of post-translational modifications, and similarly large range of effector proteins. GTPases cycle between the active guanosine triphosphate (GTP)-bound and inactive guanosine diphosphate (GDP)-bound states (Figure 5). Switching between these two states is mediated by guanine nucleotide exchange factors (GEFs) which facilitate GDP dissociation, and GTPase activating proteins (GAPs) that promote GTP hydrolysis. Alternation in Rho GTPase localization also occurs, promoted by sequestration of GDP-bound GTPases from plasma membrane to cytosol through its binding with guanine dissociation inhibitors (GDIs) which shield the former's c-terminus transmembrane domain (GTPase activation cycle detailed in [92]). Along with GEF/GAP/GDI regulation a wide array of post-translational modifications, including phosphorylation, prenylation and SUMOylation (reviewed in [93]), further actuate Rho GTPases' efficacies as general modulators of many cytoskeletal signal transductions. In terms of RhoA for example, phosphorylation at serine

188 by protein kinase A (PKA) or G (PKG) can inhibit activity by enhancing RhoA's interaction with RhoGDI [94, 95]. Furthermore, interactions of Rho GTPases with over 30 effector kinases and scaffold proteins have been suggested [96], with downstream functions such as: actomyosin organization [97] (see Section 1.1.3.2), cytokinesis [98], c-Jun N-terminal kinase (JNK) signaling [99, 100], translation regulation [101] and lipid level modulation [102-106].

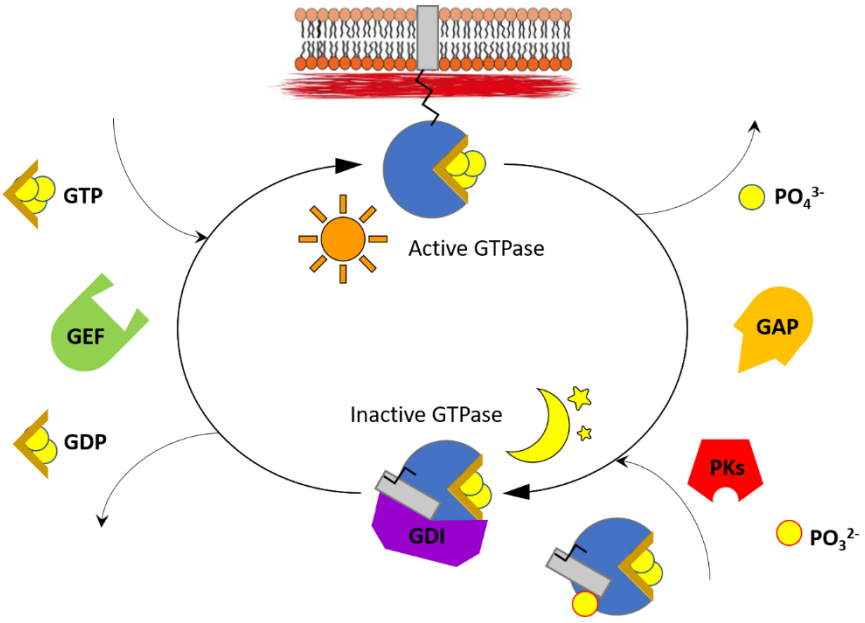

Figure 5. Regulation of Rho GTPase activation states.

Rho GTPases (blue) are active and localize at the plasma membrane when bound to GTP, while inactive and sequestered to the cytosol through GDI (purple) interaction when bound to GDP. GEFs (green) and GAPs (orange) mediate GDP dissociation and GTP hydrolysis of GTPases respectively. Rho GTPase phosphorylation by protein kinases (red) additionally promotes GTPase-GDI complex formation.

1.1.5. Factors of RhoA, Cdc42 upstream regulation

In contrast to the canonical view of wound-induced actomyosin ring closure being directed by large-scale contraction derived from coordination of Rho GTPase-regulated signal transductions (Figure 4), ring closure has also been suggested to be regulated by a Rho GTPase signaling treadmill in which waves of RhoA and Cdc42 fluxes with activity biased towards the wound edge influence closure more directly [107]. It was observed in the same study that both the actomyosin ring and Rho GTPase activity zones closed even in the absence of contraction induced by Rho inhibitor C3 exotransferase, ROCK inhibitor Y-27632 or myosin-2 inhibitor blebbistatin, albeit ~50% reduction in closure rates. These findings challenge the logically intuitive notion of ring closure being primarily mediated by contraction. More strikingly, it has been supposed that actomyosin contractile feedback contributes to properly directed organizations of RhoA and Cdc42 activity waves [107, 108]. Indeed, the processes leading to establishment of RhoA and Cdc42 activity zones have yet to be comprehensively deciphered.

The most immediate possibility of regulatory crosstalk between Rho GTPases mediating their recruitment during wound healing is not far off the mark, as such is the case in neural developmental contexts [109, 110]. However, only antagonistic signaling between RhoA and Ras-related C3 botulinum toxin substrate 1 (Rac1) has actually been directly demonstrated [111, 112], in contrast to the relatively elusive relations between RhoA and Cdc42. These considerations render the alternative prospect of a nuanced RhoA, Cdc42 recruitment mechanism to be more likely. Several factors recognized to be necessary in such a recruitment process are briefed in the following.

1.1.5.1. *Ca^{2+} influx*

Divalent calcium ions play ubiquitous signaling roles in an expansive range of cellular processes (reviewed in [113]), and its necessity equally applies in the cytoskeletal regulatory context of wound healing. High intracellular Ca^{2+} levels induce microtubule dynamics by promoting microtubule catastrophe reactions, directly destabilizing growing microtubule ends without changing its C_c [114]. Such disassembly is shortly followed by further microtubule rearrangement in the form of wound-directed elongation [115]. Less direct Ca^{2+}-induced actin dynamics also occur through troponin-binding which shifts tropomyosin position [116], sterically promoting actin-myosin interaction and contraction (reviewed in [117]). Furthermore, protein kinase C (PKC) activation promoted by Ca^{2+} has been observed to be required for RhoA-induced ROCK activation [118, 119]. Inhibition of wound closure in the absence of external Ca^{2+} has been repeatedly demonstrated in multiple cell models such as *Xenopus* oocytes [78, 79], sea urchin eggs [65, 66], rat red blood cells [120], mouse muscle fibers [121] and mouse fibroblasts [122]. In the former, wound repair perturbation upon external Ca^{2+} removal was observed to be caused by prevention of actomyosin recruitment, also seen in oocytes treated with C3 exotransferase [78]. The specific correlation of RhoA and Cdc42 activations being dependent on extracellular Ca^{2+} influx has been additionally demonstrated since [79]. However, the yet to be resolved time interval between the events, and lack of evidence in calcium's direct effects on RhoA and Cdc42, strongly suggest existence of other intermediate factors.

1.1.5.2. *Plasma membrane changes*

Considering the inevitability of lipid disruption upon cell wounding, as well as known roles of lipid-binding proteins such as profilin [123] and vinculin [102] in regulations of cytoskeletal assembly and cytoskeleton-membrane attachments, plasma membrane components have also been suspected to contribute in some capacity to the cytoskeletal reorganization aspect of wound healing. For example, phosphoinositides, phosphorylated forms of phosphatidylinositol (PI) lipids, have been demonstrated *in vitro* to promote RhoA GDP-to-GTP exchange through partial opening of the RhoA-RhoGDI complex [124]. It has more recently been observed that *Xenopus* oocyte wounding induces peripheral formations of micrometer-scale domains enriched with an array of specific lipids, namely: phosphotidylinositol 4,5-biphosphate (PIP_2); phosphotidylinositol 3,4,5-trisphosphate (PIP_3); phosphatidylserine (PS); phosphatidic acid (PA) and diacylglycerol (DAG) [125]. These domains are of interest as PS localized close to RhoA activity at the wound edge, whereas PIP_2 and PIP_3 associated with the outer Cdc42 activity zone. DAG and PA were shown to overlap RhoA and Cdc42 activity zones, experimental blocking of DAG resulting in significant wound healing failure [125]. Since DAG in particular is known to recruit PKCβ and PKCη [126], the latter two being observed to mediate Rho GTPase activation and inhibition respectively [125, 127], it has been suggested that enriched DAG at the wound site functions as an upstream lipid regulator of RhoA and Cdc42 activities. Together with the possibly subtler functions of other lipid domains [125], regulation of Rho GTPase activation by these varied lipids partially explains the flexibility of the actomyosin-mediated wound healing response. How such coordinated lipid compartmentalization occurs has yet to be elucidated.

1.1.5.3. *Local GEF/GAP regulation*

Incorporations of constitutively active (CA) or dominant negative (DN) isoforms of RhoA and Cdc42 have been observed to mutually modulate activity distribution of the other in wounded oocytes (detailed in [79]). This finding demonstrates local crosstalk between these two GTPases but, as previously alluded, was unable to resolve whether such antagonistic regulation is direct or indirect. In a later study, candidate screening of Rho GTPase activators and inhibitors led to identification of the dual RhoGEF-GAP active breakpoint cluster region-related protein (ABR) as an upstream regulator of RhoA and Cdc42 activity zones during wound healing [128]. Colocalizing with the active RhoA region, ABR's possession of both the dbl homology (DH) and GAP domains enables its concurrent regulation of RhoA activation and Cdc42 inhibition respectively. Accordingly, ABR depletion, or incorporation of DH domain-mutated ABR, severely abrogated RhoA activation [128]. Furthermore, mathematical models concluded that ABR's positive feedback with the active RhoA zone sufficiently accounts for spatial maintenance of the latter [129, 130]. However, the same models also invoke an ABR-independent feedback loop for active Cdc42's spatial bistability. It should be further noted that breakpoint cluster region-related protein (BCR), the only other currently known Rho GTPase dual GEF-GAP [131], has yet to be directly investigated in the actomyosin-mediated wound healing context.

1.1.6. Cellular tensegrity of wound healing

Another potential factor of Rho GTPase recruitment, which has often been overlooked, concerns changes to equilibrium cell tension upon wounding. According to the cellular tensegrity model (see Section 1.1.1), all phenomena encountered by cells which change its shape also involve corresponding changes in cell tension. Mechanical wounding of the plasma membrane applies to this paradigm by definition, causing transient increase of apparent membrane tension around the wound site (Figure 6). To elaborate, wound-induced Ca^{2+} influx leads to microtubule depolymerization and actomyosin contraction at and around the wound site (see Section 1.1.5.1). This combined with adhesion of affected cytoskeletal elements to membrane edges, as well as the newly created cytosolic space, results in increase of MCA forces directed away from the wound, which makes up the bulk of overall tension increase. Lipid disruption due to wounding also leads to contributing, but relatively less influential, line tension increase (reviewed in [132]). Local cell tension increase instantaneously ensues lesion widening [133], and potentially culminates in cell lysis if unobstructed.

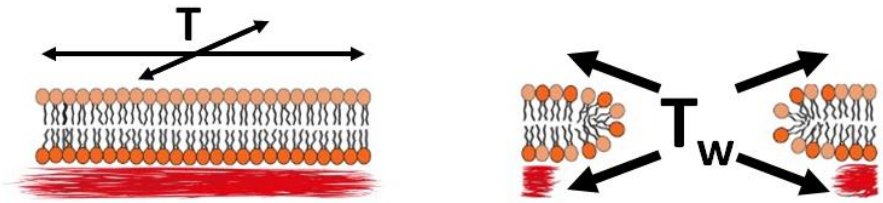

Figure 6. Biophysical consequences of mechanical wounds.

The intact cell and corresponding apparent membrane tension, *T*, enable stabilization of cellular tensile equilibrium (left). Upon mechanical wounding, the plasma membrane and underlying cytoskeleton are disrupted, resulting in compromise of said equilibrium through transient local tension increase, T_w (right).

1.2. Project description

1.2.1. Rationale

Cells respond to disruptive mechanical forces through spatiotemporal organization of F-actin, myosin, and microtubules (see Section 1.1.2), which constitute cytoskeletal dynamics that direct processes such as actomyosin-mediated wound healing. Formation and contraction of the actomyosin ring is controlled by wound peripheral activities of Rho GTPases RhoA and Cdc42 (see Section 1.1.3.2), and their recruitments have previously been demonstrated to be dependent on Ca^{2+} influx, plasma membrane lipid domains, and GEF/GAP regulation (see Section 1.1.5). However, the mechanical cue initiating actomyosin ring activity has yet to be identified.

With cellular tensegrity's application to wound healing (see Section 1.1.6), it is plausible to suppose that the cell interprets its wound-induced loss of cell tension homeostasis as an alarming mechanical signal, which causes it to spring into action. Temporary tension increase induced by membrane depletion has been observed to be the coordinating factor of morphogenic processes like cell migration [134, 135] and spreading [136]. Similar tension increases have also been suggested to promote pseudopod extension during phagocytosis [137]. These tension-dependent processes are examples of mechanotransduction, which couples active sensing of mechanical cues with transduced intracellular biochemical signaling pathways resulting in cellular response (reviewed in [138]). Perhaps actomyosin ring contraction during wound healing is triggered much the same way, considering that actomyosin contractility-derived tension counters wound-induced local tension increase. Indeed, modulation of cell tension via hyperosmotic treatment correlated with changes in Rho, Cdc42 and Rac activities [139, 140]. However, to what extent cell tension affects Rho GTPase regulation of actomyosin-mediated wound healing has not been directly

studied. Therefore, the question arises: Does local cell tension increase influence regulation of wound healing (Figure 7)?

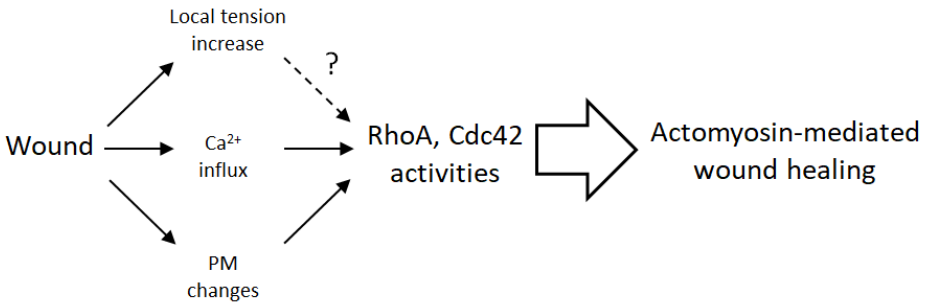

Figure 7. Local tension increase: Additional wound healing factor?

1.2.2. Hypothesis

The potential of tensile forces being an additional wound healing factor was explored in this study, based on the hypothesis that: *"Transient local tension increase is necessary for actomyosin-mediated wound healing."*

1.2.3. Research objectives

The following research objectives set the foundation for a series of cell microindentation, confocal microscopy, and western blot experiments:

Objective 1 – Verify and quantify osmotically driven cell tension reduction

Xenopus oocytes were subjected to hyperosmotic sucrose media incubation, which was expected to negatively affect their equilibrium level of apparent membrane tension (Figure 8). This cell tension reduction was quantified through comparative microindentation.

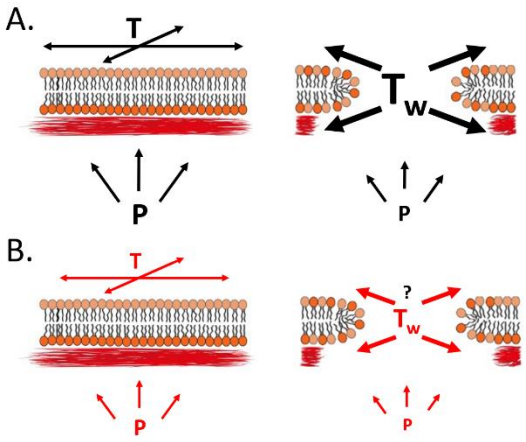

Figure 8. Osmotically driven cell tension decrease.

(A) Isotonic cells undergo wound-induced transient local tension increase, T_w. **(B)** In contrast, cells subjected to hyperosmotic treatment lose cell volume, resulting in decrease of hydrostatic pressure, *P*, negatively affecting the equilibrium level of cell tension, *T*. Cell tension reduction is presumed to inhibit local tension increase upon wounding.

Objective 2 – Determine cell tension reduction's influence on actomyosin-mediated wound healing

Sucrose-treated oocytes were utilized in time lapse confocal microscopy experiments to determine whether cell tension reduction perturbs actomyosin-mediated wound healing as expected.

Objective 3 – Investigate cell tension reduction's influence on RhoA, Cdc42 regulation of actomyosin-mediated wound healing

Sucrose-treated oocytes underwent further confocal microscopy experiments as well as western blotting and Rho GTPase activity assays to investigate how cell tension decrease affects RhoA, Cdc42 activities and their regulation of actomyosin activity. It was expected that cell tension decrease inhibits RhoA and Cdc42 activities, in turn causing perturbed wound healing (Figure 9).

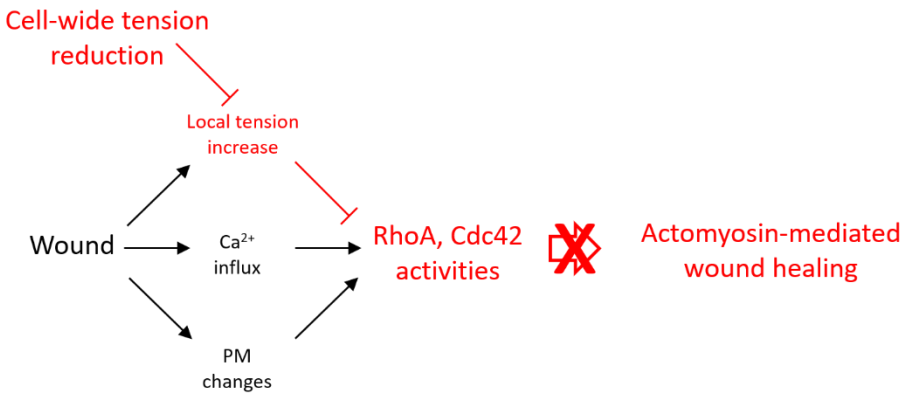

Figure 9. Experimental design: Cell-wide tension reduction.

Insights gained from achieving these research objectives expand the basic scientific knowledge of cell tension's influence in cell contractile processes, which can be further applied to the fields of cell wound healing and division.

Chapter 2:
Materials and Methods

2. Materials and Methods

2.1. Animal housing

Adult female *Xenopus laevis* frogs (Nasco, USA) were housed in plastic tanks at a density of up to 12 frogs per tank. Frogs were kept as per standard operating procedures (SOPs) determined by McGill University Ethics and Compliance. Briefly, frogs were kept on 12 hour light/12 hour dark cycles at 18°C. Frogs were fed Nasco frog brittle (Nasco, USA) twice a week. Housing tanks were cleaned, and the water replaced twice a week after feeding.

2.2. Oocyte collection and processing

Xenopus oocytes were surgically collected from adult females in accordance with McGill SOPs. Briefly, frogs were anesthetized in a 1g/L, pH 7.0 ethyl 3-aminobenzoate methanesulfonate solution for 20 minutes immediately before surgery. Following surgery, frogs were left to rest for at least 3 months. Each frog underwent a maximum of 3 separate surgeries. Collected oocytes were stored in pH 7.4 Oocyte Ringer-2 solution (OR-2; 82.5mM NaCl, 2.5mM KCl, 1mM CaCl2, 1mM MgCl2, 1mM Na2HPO4, 5mM HEPES). Collected ovaries were carefully cut into smaller chunks, then incubated in 0.15% collagenase type II in OR-2 solution for 75 minutes at room temperature, then blocked for 1 minute with 5% BSA in OR-2 solution, then rested in OR-2 at 16°C for at least 2 hours. After rest, stage VI oocytes were manually defolliculated using a pair of watchmaker forceps under a binocular microscope. For lysate processing, 100 oocytes incubated with each sucrose media solution (see Section 2.3) were lysed in 150ul of lysis buffer (150mM NaCl, 5mM $MgCl_2$6H2O, 20mM HEPES, 1% Triton X-100, 1mM PMSF, 0.2μM Aprotinin, 10μM Leupeptin, 1mM DTT, 10% PhosSTOP) through vigorous mixing by pipetting with cut tips in 1.5ml tubes.

Lysates were then centrifuged at 16k rpm in 4°C for at least 20 minutes, then the aqueous cytoplasmic fraction aliquoted into new 1.5ml tubes for further analysis. Lysate samples used at later dates were stored in -80°C.

2.3. Cell tension reduction

To reduce overall cell tension, defolliculated oocytes were incubated in 0mM (control), 50mM, 150mM, and 250mM solutions of sucrose in OR-2 media for 30 minutes at 16°C with agitation. These conditional oocytes were then further processed for additional experimental methods.

2.4. Microindentation

Oocytes were compressed with a custom microindenter setup consisting of the oocyte, supported on a leveled lab jack, in contact with a 2.5mm-diameter, polylactic acid cylindrical probe attached to a load cell (Futek #LRF400), which was affixed on a micromanipulator (Sutter Instrument #MP-285; Figure 10A). Control of micromanipulator movement and data acquisition were performed through MATLAB programming. Individual oocytes were subjected to one of two compression regimes; they were either compressed until rupturing for rupture measurements (Figure 10B, C) or compressed 20% of rupture for elastic measurements (Figure 10D, E). Rupture measurements were necessary to perform elastic compressions comparable across conditions, since sucrose media-incubated oocytes were osmotically precompressed prior to their microindentation (see Section 3.1). The load cell measured oocyte tension exerted onto the probe every 10μm of displacement. Oocyte elasticity was measured through Young's modulus (*E*), which was calculated by solving the Hertz equation of non-adhesive elastic contact (Figure 10F) with the inputs of force (*F*),

distance (h), probe radius (R = 0.00125m), and Poisson's ratio (v = 0.5). Calibration of the load cell was performed between every few experimental sessions by compressing the probe on a scientific scale, then adjusting the calibration ratio on MATLAB code.

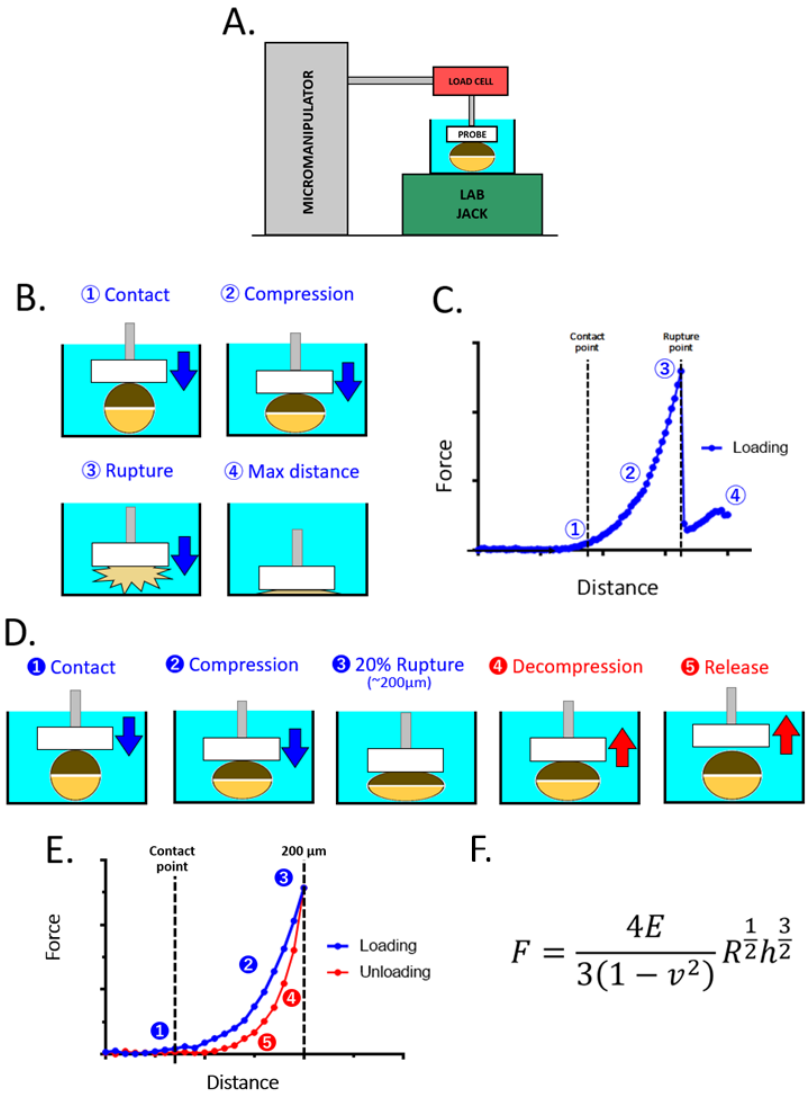

Figure 10. Comparative rupture and elastic microindentations.

(A) Schematic of microindenter setup. **(B)** Major stages of an oocyte undergoing compression until rupture and **(C)** a representative force-distance curve of its measurements, key parameters of which were compared. **(D)** Major stages of oocyte elastic compression and **(E)** a resulting force-distance curve. **(F)** The Hertz equation of contact mechanics used to derive Young's modulus, E.

2.5. Western blot, Rho GTPase activity assays

Oocyte lysate proteins (see Section 2.2) were electrophoretically separated using 10% SDS polyacrylamide gels from the TGX Stain-Free FastCast Acrylamide Kit (Bio-Rad #161-0183). Separated gels were exposed to 45 seconds of UV for stain-free imaging prior to PVDF membrane transfer. Protein transfers onto PVDF membranes were performed as per system protocol of the Trans-Blot Turbo Transfer System (BioRad #1704150). Membranes were then blocked in 5% skim milk in tris-buffered saline (pH 7.5 TBS; 1M Tris, 1.5M NaCl) containing 0.1% Tween-20 (TBS-T) solution for 2 hours at room temperature, then incubated overnight at 4°C with one of the primary antibodies rabbit anti-RhoA (1:500, Santa Cruz #sc-179), rabbit anti-p-RhoA (1:1000, Santa Cruz #sc-32954), mouse anti-Cdc42 (1:500, Cytoskeleton #ACD03), or rabbit anti-GAPDH (1:10000, Abcam #ab9485), washed with TBS-T, followed by incubation with the corresponding goat anti-rabbit or goat anti-mouse secondary antibodies (1:50000, Jackson Laboratory) for 1 hour at room temperature, washed with TBS-T, then detected using Clarity Max Western ECL Substrate (Bio-Rad #1705062). All primary and secondary antibody solutions were diluted in 2.5% skim milk in TBS-T solution. Protein blot images were obtained with the ChemiDoc Touch imaging system (Bio-Rad #17083370) and analyzed using Image Lab software (Bio-Rad). Stripping of PVDF membranes was performed by incubating them in 10% glacial acetic acid in TBS-T solution for 30 minutes at room temperature, then membranes underwent procedures as described above to obtain analogous data for GAPDH loading control.

For Rho GTPase activity assays, oocyte lysate protein samples enriched for the active GTP-bound forms of RhoA and Cdc42 were prepared utilizing the Rhotekin-RBD-GST (Cytoskeleton #RT02) and PAK-GST protein beads (Cytoskeleton #PAK02), respectively. Briefly, 25µl of loading buffer (15mM EDTA), then 2.5µl of MilliQ water or GTPγS (positive control) were added to 250µl of

oocyte lysate, then incubated at room temperature for 15 minutes. 28µl of stop buffer (60mM $MgCl_2$) was added, then mixed by pipetting. 20µl of the corresponding beads were then added, carefully mixed by pipetting with a cut tip, then incubated at 4°C for 1 hour. Samples were then spun at 5k rpm for 5 minutes at 4°C, the supernatant aspirated, and remaining sample washed with 500µl wash buffer (25mM pH 7.5 Tris-HCl, 30mM $MgCl_2$, 40mM NaCl). This washing procedure was repeated 3 times. Samples were then resuspended in 2X Laemmli buffer and subsequently processed for western blot analysis.

2.6. Molecular probe microinjection

Oocytes were injected with ~2nl of one of the molecular probes tracking actin (Alexa568-G-actin), rhotekin GTPase binding domain (pCS2-eGFP-rGBD), or N-WASP GTPase binding domain (pCS2-GFP-wGBD) [79] using pulled microneedles via pico injector (Harvard Apparatus #PLI-100). Injected oocytes were rested in OR-2 at 16°C for at least 12 hours, except for those injected with Alexa568-G-actin which were rested for several hours, before further use in microscopy analysis.

2.7. Confocal fluorescence microscopy

Confocal fluorescence microscopy was performed with a Quorum WaveFX-X1 spinning disk confocal system, on a Leica DMI6000B inverted microscope. Samples were observed with 40X/0.85 dry DIC and 63X/1.4 oil DIC objective lenses. Live oocytes were wounded with a ~25µm diameter laser using the Andor MicroPoint laser system (2 pulses, 50% transmission intensity). Hamamatsu "ImagEM" EM-CCD cameras were used to capture images of fixed oocyte

samples, as well as live oocyte membrane topography and wound sites at 30s intervals (200ms exposure, 200 EM gain). Data was acquired with the MetaMorph Quorum WaveFX software.

2.8. Statistics

Ordinary one-way ANOVAs with Dunnett's tests for multiple comparisons across conditions were performed to analyze oocyte rupture and elastic metrics, as well as lysate blot densitometries. Normal distributions of all data sets were confirmed with Shapiro-Wilk tests. Significance was set at $p<0.05$.

Chapter 3:
Results

3. Results

3.1. Cell tension reduction through sucrose media incubation

To investigate cell tension's influences on wound healing and its regulation, the equilibrium apparent membrane tension of *Xenopus* oocytes was independently modulated. Reduction of cell-wide equilibrium tension was experimentally achieved through cell incubation in hyperosmotic sucrose media (Figure 8). To initially verify and quantify osmotically driven cell tension reduction, unwounded oocytes underwent comparative rupturing and elastic microindentations shortly after hyperosmotic treatment.

Oocytes incubated in sucrose media of various concentrations were first microindented until rupturing (Figure 10B, C). To characterize oocyte rupture metrics, various parameters of the resulting force-distance curves were measured (Figure 11). Oocytes incubated in control media withstood 353 ± 25μm of compression, exerting 4.41 ± 0.83 millinewtons (mN) immediately before rupture. They were observed to do 48.7 ± 10.2 arbitraty units (a.u.) of work in this period.

Upon comparing metrics between control and sucrose-treated oocytes, it was first observed that sucrose media-incubated oocytes contacted the microindenter probe and ruptured at significantly greater distances, in dose-dependent manners (Figure 11A, B). This suggests that sucrose media incubation induced cell shape change into oblate spheroids relative to control, graphically represented by consistent rightward shifts of corresponding force-distance curves along the distance x-axis (Figure 12). Considering its dose-dependent nature, such morphology change is likely a consequence of hyperosmotic precompression through cell volume loss and hydrostatic pressure decrease, resulting from water efflux.

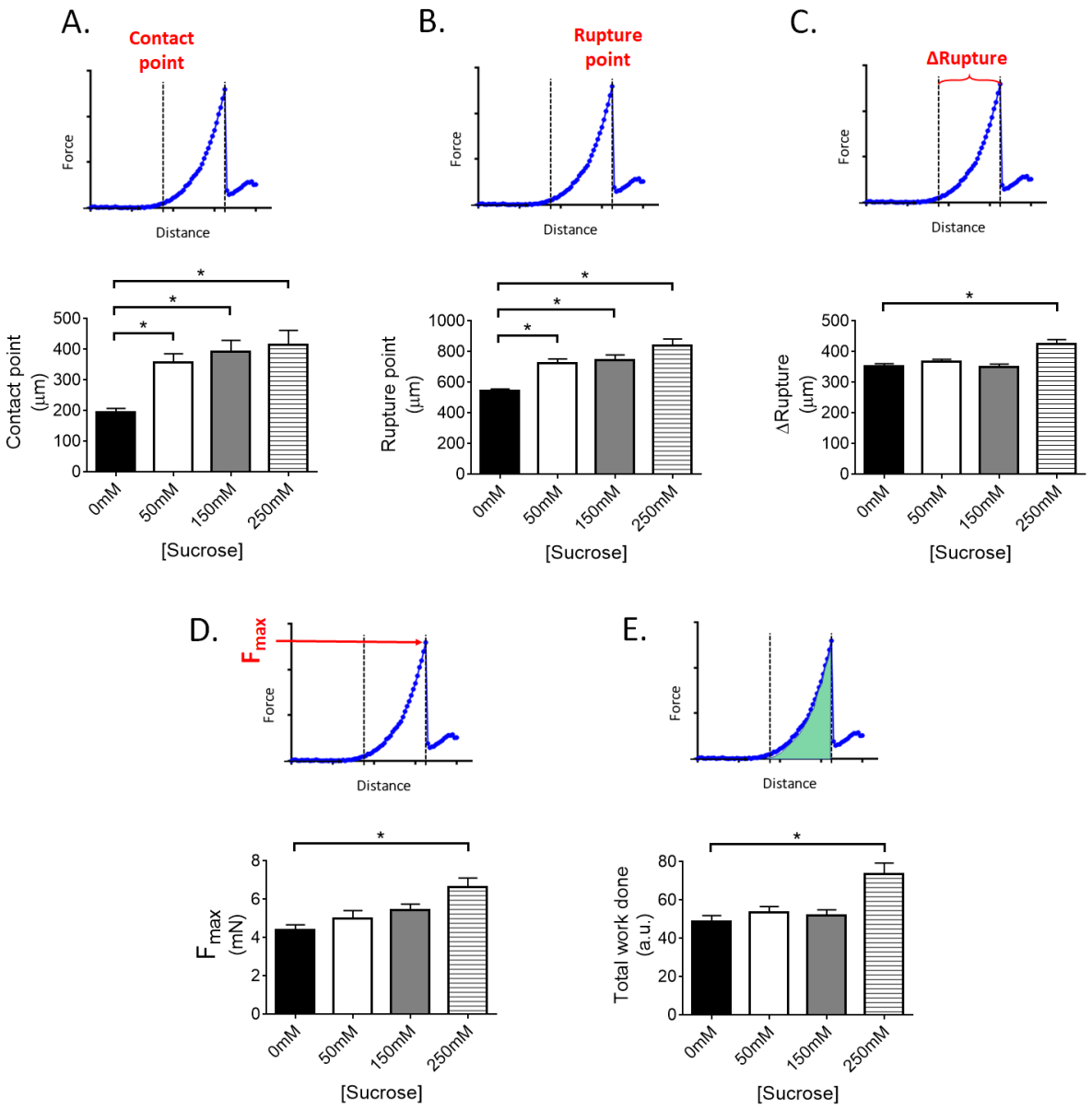

Figure 11. Sucrose media incubation modulates rupture parameters of oocytes.

Various parameters were compared across conditional oocytes to characterize their biomechanics as they succumbed to rupture, those being: **(A)** Distance point of initial oocyte-probe contact, **(B)** distance point of oocyte rupture, **(C)** total compression distance before oocyte rupture (ΔRupture), **(D)** oocyte tension at rupture point (F_{max}), and **(E)** total work done by the oocyte (area under curve). mN = millinewtons, a.u. = arbitrary units. Mean ± SEM, n = 10, $p<0.05$.

In addition to shape change, oocytes incubated in sucrose media of the highest concentration also withstood greater distances of compression (424 ± 49μm; Figure 11C) and exerted more force immediately prior to rupture (6.66 ± 1.43mN; Figure 11D). This was supported by the further observation of these oocytes performing more work on the probe (73.6 ± 18.3 a.u.; Figure 11E).

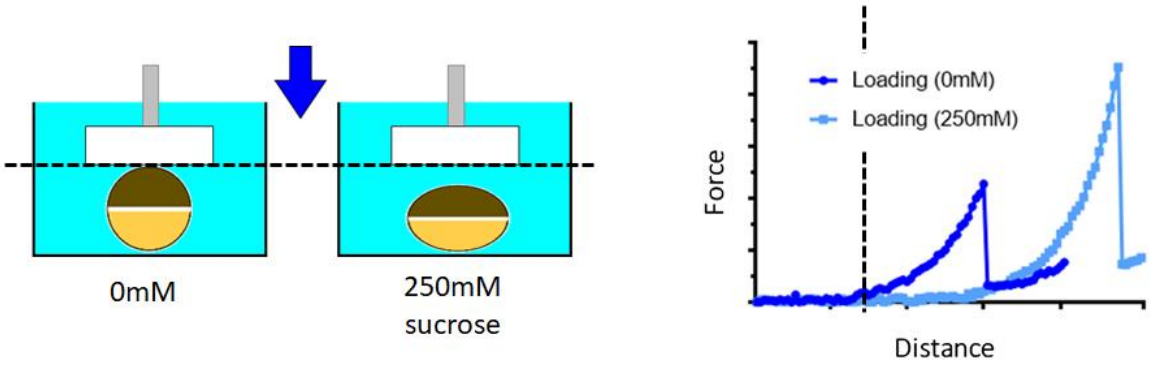

Figure 12. Cell shape change upon sucrose media incubation.

Sucrose media-incubated oocytes had morphological changes, being oblate spheroids relative to control (left). Accordingly, these oocytes consistently contacted the probe significantly later than control oocytes (right).

Based on data from their rupturing (Figure 11), oocytes were then microindented by distances relative to 20% of their rupture and decompressed (Figure 10D, E) to characterize their elasticities. Oocyte Young's moduli were derived by inputting total oocyte deformation and distance of oocyte-probe contact, along with the probe radius (Figure 13). Control oocytes deformed by 2.73 ± 0.43 a.u. over 278 ± 8 μm of probe contact, leading to a calculated Young's modulus of 1.75 ± 0.15 kilopascals (kPa). This is within the typical modulus values of cells, ranging from a few hundred pascals to tens of kPa [141], and similar to those of aged mouse oocytes (1.6 ± 0.4 kPa) [142].

In comparison, it was observed that sucrose media-incubated oocytes underwent similar magnitude of deformations to control (Figure 13A), but while in contact with the probe for less distances (Figure 13B), resulting in significant decrease of the former's Young's moduli (Figure 13C). Oocytes incubated in the highest concentration of sucrose media had an approximate twofold reduction of Young's moduli compared to control (0.85 ± 0.11kPa). In other words, oocytes treated with sucrose media incubation are indeed less stiff.

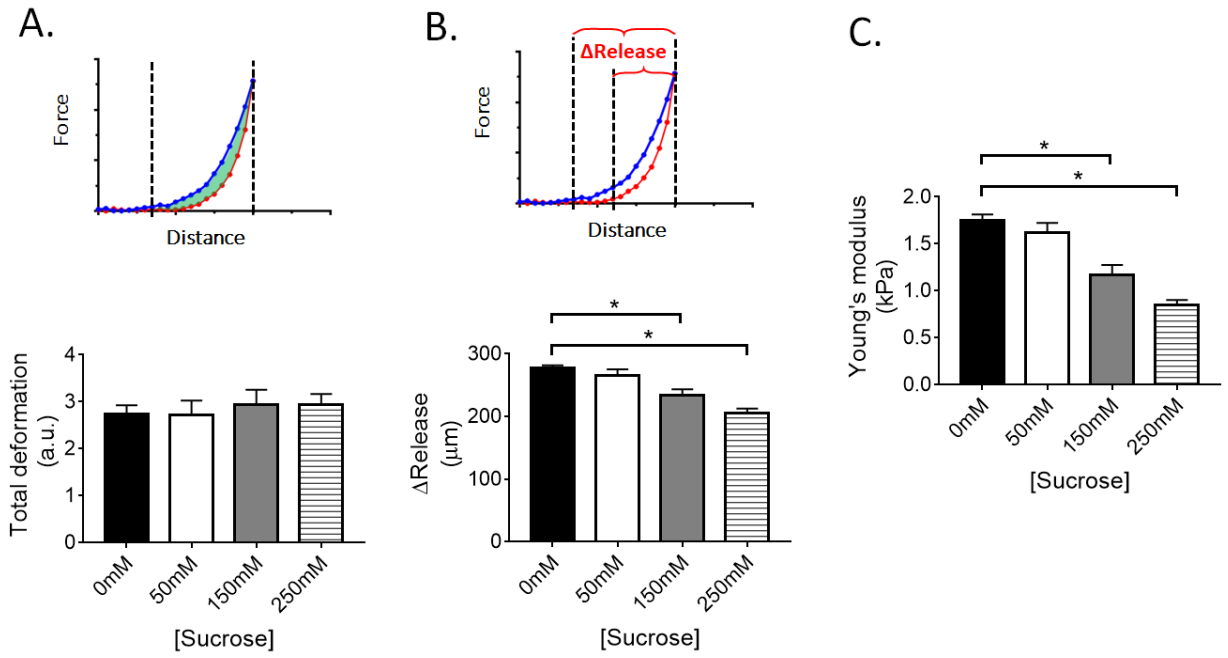

Figure 13. Sucrose media-incubated oocytes are significantly less elastic.

(A) Total oocyte deformation (area between curves), and **(B)** total distance of oocyte-probe contact (ΔRelease) were two of the metrics used to calculate **(C)** Young's moduli of conditional oocytes. a.u. = arbitrary units. Mean ± SEM, n = 5, $p<0.05$.

3.2. Wound healing rate decrease in sucrose-treated oocytes

In the model of this study, sucrose-treated oocytes are presumed to have inhibited wound-induced local transient tension increase which is hypothesized to be a necessary factor for actomyosin-mediated wound healing (Figure 9). To determine whether cell tension reduction perturbs wound repair, oocytes were microinjected with fluorophore-conjugated G-actin (Alexa568-G-actin) to track *de novo* actin polymerization. Prior to wounding, cell tension reduction appears to increase intensity of cortical actin, but overall network topology looks largely unaffected (Figure 14).

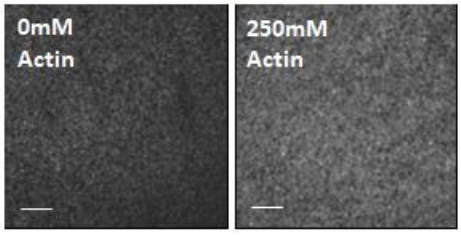

Figure 14. Cortical actin intensity increase upon cell tension reduction.

Confocal images of F-actin fluorescence in oocytes injected with Alexa568-G-actin. Oocytes incubated in 250mM sucrose media appear to have increased intensity, but little change in overall topology, of cortical actin cytoskeleton. Scale bar = 10μm.

Oocytes were then wounded via laser ablation and observed over time, compared between the most severely treated and control oocytes. Sucrose-treated oocytes had dramatically less local actin enrichment peripheral to the wound site, while concentric enrichment is clearly seen in control oocytes by 3 minutes after wounding (Figure 15A). Additionally, wound healing in sucrose-treated oocytes was disturbed even 8 minutes after wounding, in contrast to the ring being close to full constriction in control oocytes. This difference in local actin enrichment suggests changes in actin recruitment as the cause of perturbed wound healing induced by cell tension reduction. It should

also be noted that sucrose-treated oocytes still exhibited plasma membrane dynamics after wounding (Figure 15B).

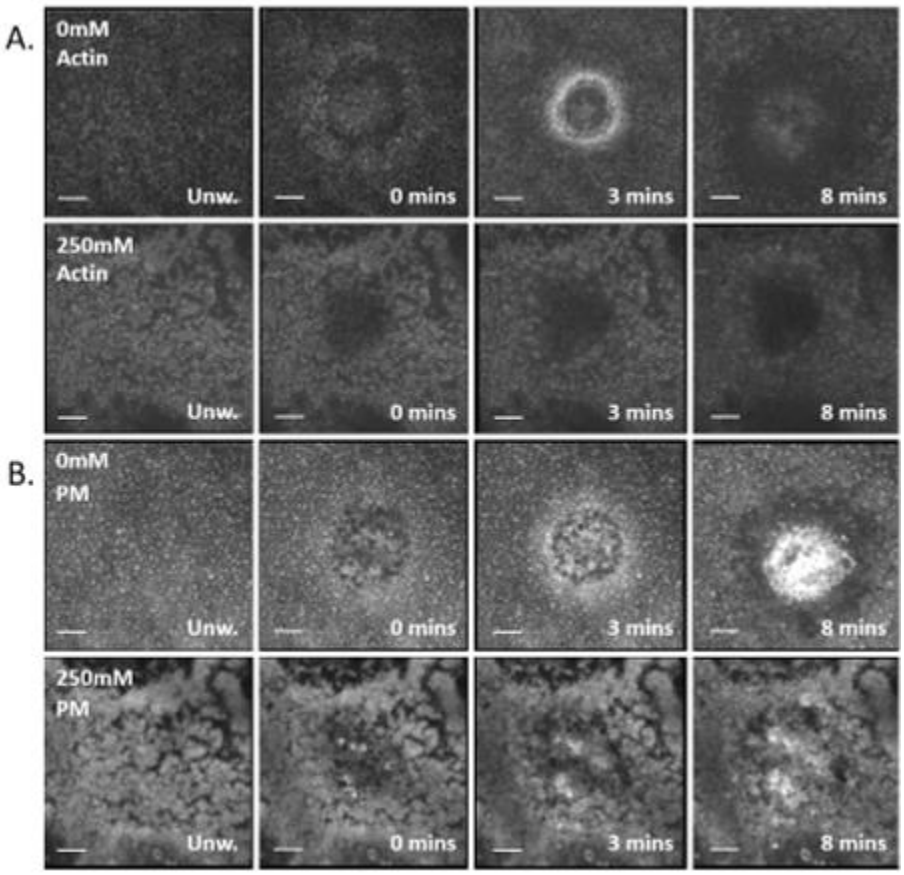

Figure 15. Decreased local actin enrichment, healing rates in sucrose-treated oocytes.

(A) Confocal images of F-actin fluorescence in oocytes injected with Alexa568-G-actin. Oocytes incubated in 250mM sucrose media have little wound-peripheral actin enrichment and decreased wound healing rates. **(B)** Sucrose-treated oocytes displayed wound-induced plasma membrane dynamics, as observed via CellMask. Unw. = unwounded. PM = plasma membrane. Scale bar = 10μm.

3.3. Rho GTPase activity changes in sucrose-treated oocytes

The Rho GTPases RhoA and Cdc42 regulate local recruitment of actin in response to cell wounding (see Section 1.1.3.2), which appears to be negatively affected in sucrose-treated oocytes. To investigate cell tension reduction's influence on Rho GTPase regulation of actomyosin-mediated wound healing, RhoA and Cdc42 activities were compared between control and sucroses-treated oocytes.

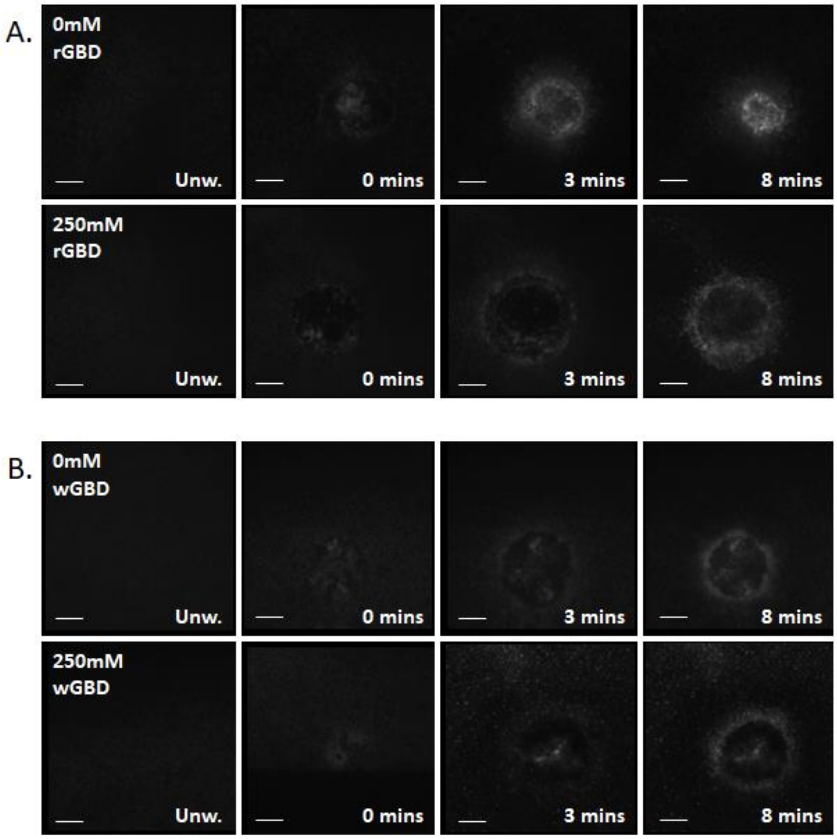

Figure 16. Decreased RhoA, unchanged Cdc42 activities in sucrose-treated oocytes.

(A) Confocal images of fluorescence in oocytes injected with pCS2-eGFP-rGBD. Oocytes incubated with 250mM sucrose media have reduced enrichment of active RhoA around the wound. **(B)** Contrastingly, tension reduction appears to have little effect on active Cdc42 recruitment, as observed via pCS2-GFP-wGBD. Unw. = unwounded. Scale bar = 10μm.

To study wound peripheral activities, oocytes were microinjected with the pCS2-eGFP-rGBD and pCS2-GFP-wGBD molecular probes. Corresponding GFP fluorescence enabled visualization of the concentric RhoA, Cdc42 activity zones during oocyte repair of laser-induced wounds. Concentric active RhoA recruitment to the wound periphery was negatively affected by cell tension reduction (Figure 16A) This inhibition of local RhoA activity correlates with disrupted local actin recruitment in sucrose-treated oocytes. Contrastingly, local recruitment of Cdc42 appeared to be largely unaffected by cell tension reduction (Figure 16B).

To compare cell-wide RhoA and Cdc42 activities, lysates of unwounded oocytes were analyzed for expression levels. Relatively stable expressions of total RhoA (Figure 17A) and Cdc42 (Figure 17B) were observed across all sucrose media conditions, albeit a somewhat upward trend of Cdc42 total levels (Figure 17B, right). In contrast, levels of active GTP-bound RhoA and Cdc42 were significantly modulated upon cell tension reduction. The most severely treated oocytes had an approximate twofold decrease of RhoA activity (Figure 17C) and increased Cdc42 activity by around threefold (Figure 17D).

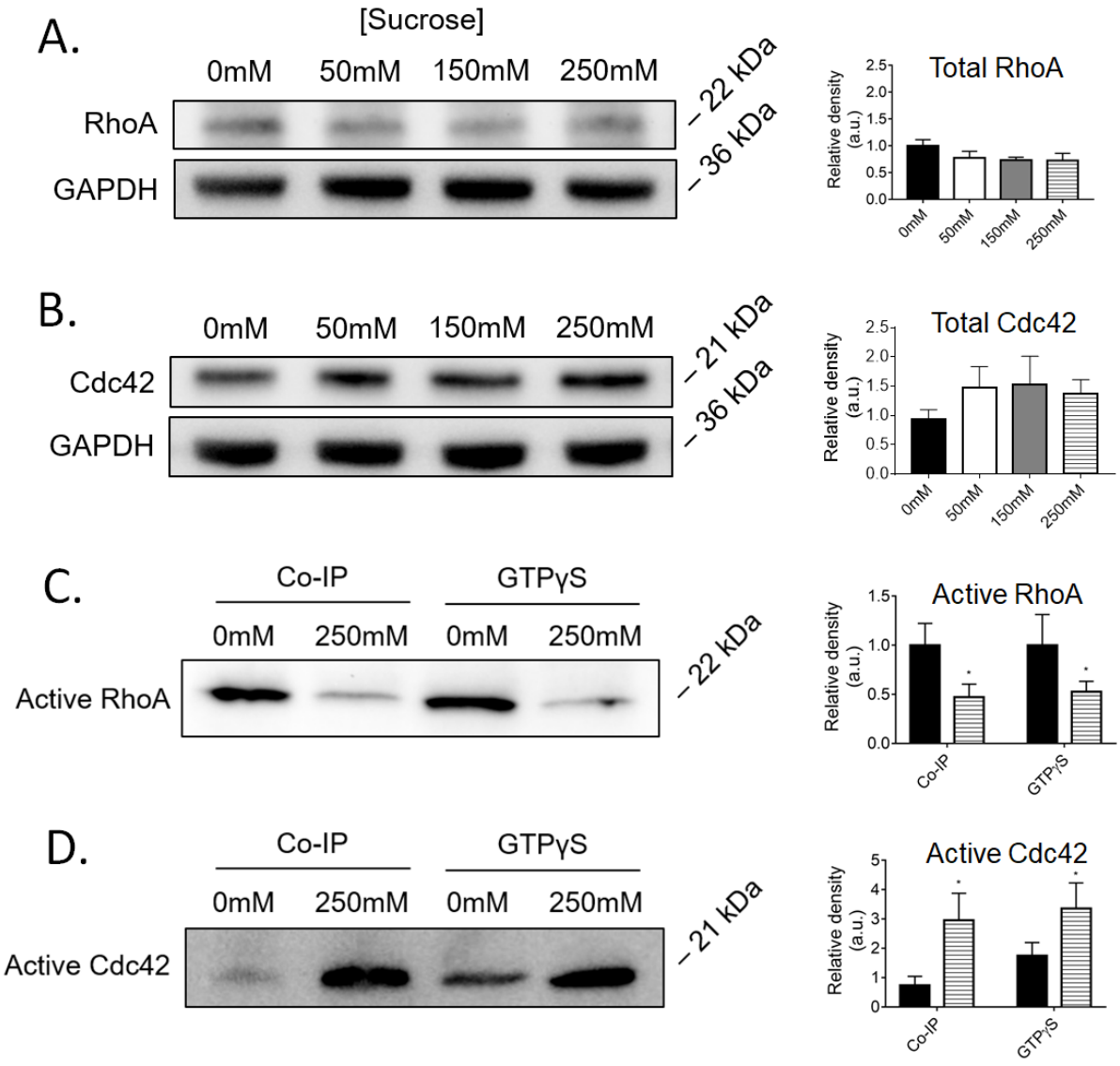

Figure 17. Cell-wide decreased RhoA, increased Cdc42 activities in sucrose-treated oocytes.

Lysates of 100 unwounded oocytes incubated in sucrose media of various concentrations were blotted for expression levels of: **(A)** Total RhoA, **(B)** total Cdc42, **(C)** active RhoA, and **(D)** active Cdc42. a.u. = arbitrary units. Mean ± SEM, n = 5 for densitometric quantifications at right. $p<0.05$

In light of correlative local actin recruitment and RhoA activity inhibitions upon cell tension reduction, the latter's regulation was further investigated. It has previously been demonstrated that RhoA's phosphorylation at serine 188 by protein kinases can inhibit RhoA activity by enhancing its interaction with RhoGDI (see Section 1.1.4). To determine whether RhoA activity was inhibited through serine 188 phosphorylation resulting from cell tension reduction, oocyte lysates were additionally blotted and analyzed for phosphorylated RhoA (p-RhoA) expression. Treated oocytes had similar expression levels of p-RhoA to control (Figure 18), suggesting RhoA phosphorylation is not playing a role in cell tension reduction's RhoA inhibitory effects.

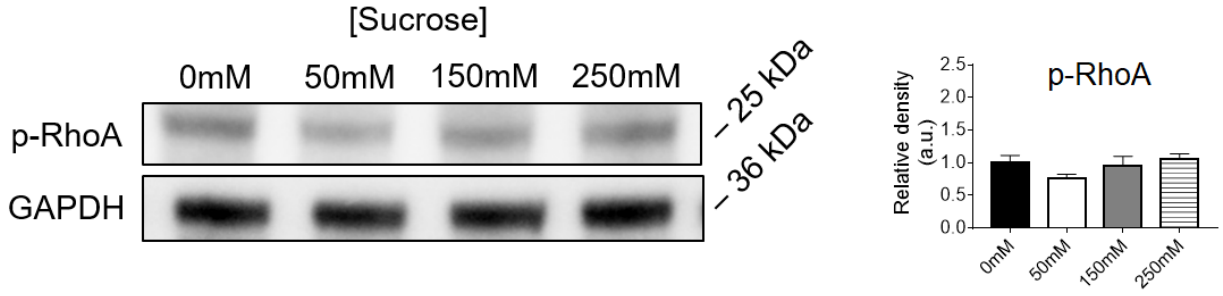

Figure 18. Tension reduction induced no changes in levels of cell-wide p-RhoA.

Lysates of 100 unwouded oocytes incubated in sucrose media of various concentrations were blotted for p-RhoA and analyzed. a.u. = arbitrary units. Mean ± SEM, n = 5 for densitometric quantifications at right.

Chapter 4:
Discussion

4. Discussion

4.1. Discussion of major findings

Xenopus oocytes incubated in sucrose media were less stiff in a dose-dependent manner. Indeed, the most severely treated oocytes had significant reduction of Young's moduli (Figure 13C) and performed more work (Figure 11E) compared to control. This demonstrates hyperosmotic media incubation as a proven method of cell tension reduction. That said, hyperosmotic treatment was subjected on unwounded oocytes, and its induced cell tension reduction was not directly measured at the wound site (see Section 4.2.2). Consequently, osmotically driven cell tension reduction was only assumed to inhibit wound-induced transient local tension increase.

Sucrose-treated oocytes which were wounded had disturbed local actin enrichment and decreased wound healing rates (Figure 15). Inhibition of wound peripheral RhoA activity upon cell tension reduction (Figure 16A) is probably the primary cause of observed actomyosin-mediated wound healing perturbation. This critical correlation elucidates actomyosin's mechanotransducive behavior in response to mechanical wounds. However, the specific mechanism of RhoA activity inhibition has yet to be determined (see Section 4.4.3). Furthermore, in contrast to observed RhoA activity inhibition in sucrose-treated oocytes, it was found in an earlier study that hyperosmotic stress activated Rho in LLC-PK_1 porcine kidney cells [140]. Even so, this was observed on epithelial cells with direct cell-cell and cell-extracellular interactions, unlike oocytes. These cell adhesions likely play additionally significant roles in Rho GTPase-mediated mechanosensation which were not explored in this study (see Section 4.2.1).

Cell tension reduction's promotive effects on Cdc42 activity are less clear, particularly in the wound healing context. Hyperosmotic treatment was previously observed to promote Cdc42

activity and subsequent cytoskeletal reorganization in CHO cells [139]. It was postulated that osmotically driven cell volume reduction leads to mechanical activation of Cdc42 signal transduction, which in turn increases cell-wide submembraneous F-actin assembly. Such mechanical Cdc42 activation is consistent with the increased intensity of overall cortical actin cytoskeleton (Figure 13), as well as the promoted activity of Cdc42 in whole-cell lysates of sucrose-treated unwounded oocytes (Figure 15B). However, influence of cell tension on local Cdc42 activity around wounds should be investigated further. Nonetheless, observations made in this study demonstrate the tension sensitivity of Rho GTPases in cell morphogenic control of wound healing.

4.2. Experimental limitations

4.2.1. Xenopus oocyte as single-cell model

Xenopus laevis oocytes were utilized in this study due to their large size, high level of manipulability, and wealth of past experiments in the actomyosin-mediated wound healing context. However, there are also intrinsic limitations in *Xenopus* oocytes as a single-cell model. Its lack of adhesive contacts with other cells and the extracellular milieu ignores RhoA's demonstrated regulations of cell junction dynamics [143] and integrity maintenance [144], which may also be influenced by cell tension. This limits application into adherent cell models, which are the foundation of cell migration studies. In addition, usage of non-mammalian oocytes led to technical difficulties when performing western blots (see Section 4.2.4), as well as a fundamental issue of to what extent the studied processes are evolutionarily conserved in somatic cells. Indeed, organized actomyosin ring formation and contraction during wound healing of mammalian somatic cells remain to be confirmed.

4.2.2. Hyperosmotic media incubation as cell tension reduction model

Incubation in hyperosmotic media conclusively reduces cell tension, but does so across the whole cell. This study did not directly modulate cell tension locally around the wound site, which should be done to directly confirm its expected inhibition of wound-induced local tension increase. In addition, cellular changes in response to hyperosmotic stress are vast (reviewed in [145]). In particular, stress-induced mitochondrial dysfunction [146] may be independently perturbing wound repair, since mitochondria have recently been suggested to play a role in wound-induced RhoA activation via mitochondrial redox signaling [147]. Therefore, more direct mechanical methods of cell tension modulation should be additionally performed to definitively decouple cell tension's influence on wound healing (see Section 4.4.2).

4.2.3. Cell tension measurement via microindentation

Oocyte microindentation through parallel plate compression was performed (see Section 2.4) to measure oocyte biomechanics. With an observed maximum resolution in the micronewtons, this microindentation method was somewhat limiting when measuring elasticity. Such was the case when no significant differences in Young's moduli were observed in oocytes treated with numerous cytoskeletal stabilizing and destabilizing drugs (Data not shown). That said, the measured Young's modulus in (defolliculated) control oocytes was similar to those previously measured in aged mouse oocytes [142], and about $1/10^{th}$ that of mouse oocytes with the zona pellucida [148]. Furthermore, the maximum pressure exerted by control oocytes calculated from force (0.898kPa) also largely agree with earlier results [149]. However, the Hertzian non-adhesive contact model used in this study was not the most accurate, considering possible adhesive contacts

of the plasma membrane and differences in actual contact area made with the probe. Utilizing higher resolution methods of microindentation such as atomic force microscopy (AFM), then calculating Young's moduli with other equations such as that of the Johnson-Kendall-Roberts (JKR) contact model may lead to additional insights on cell elasticity change, particularly those treated with cytoskeletal drugs.

4.2.4. GBD probes as fluorescent reporters of local RhoA, Cdc42 activities

The molecular probes used to track wound peripheral RhoA and Cdc42 activities (see Section 2.6) do not directly measure localizations of active RhoA and Cdc42, but those of downstream effectors rhotekin and N-WASP respectively. Nonetheless, these GTPase binding domain (GBD) probes are an improvement on earlier reporters consisting of Rho GTPases being directly tagged with fluorescent proteins which affected endogenous protein localizations [150]. GBD probes have been the gold standard tools for live imaging of Rho GTPase activities in *Xenopus* studies of wound healing, cytokinesis, cell junctions, and other facets of contractile dynamics (reviewed in [151]). It should still be noted that new probes of other Rho GTPase effectors should be developed to further demonstrate wound-induced local RhoA and Cdc42 activities, as well as improve general characterization of Rho GTPase functions.

4.2.5. Western blot analyses of lysates of unwounded oocytes

Oocyte lysates were comparatively analyzed to investigate changes in cell-wide levels of RhoA and Cdc42 activity induced by cell tension reduction, but these lysates were of unwounded oocytes. The activity assays thus do not represent the true cell-wide analog of wound-induced local Rho

GTPase activities influenced by cell tension reduction. Cell tension's influence on cell-wide Rho GTPase activities could be directly analyzed through lysates of wounded oocytes, but such lysates were not prepared in this study due to its extreme labor intensity. Also, western blot analyses were performed with the established anti-RhoA and anti-Cdc42 antibodies, which react most competently with mammalian cells (see Section 2.5). This resulted in blots having different band sizes along with those specific to RhoA and Cdc42. Such non-specificity has been similarly observed in other *Xenopus* Rho GTPase activity studies (e.g. see Supporting information of [152]).

4.3. Potential implications

4.3.1. Other fields of cytoskeletal dynamics

Actomyosin dynamics are involved in numerous other cellular processes besides wound healing such as cell division, differentiation, and migration. Wound-induced actomyosin ring contraction could be utilized to model cytokinesis (reviewed in [153]) due to similarities in their contractile activities and Rho GTPase gradients [154]. Formation and constriction of the cytokinetic ring which controls cleavage furrow ingression greatly resembles wound-induced actomyosin ring structure and function (reviewed in [155]). Considering hyperosmotic cell tension reduction was observed to change cell shape, reduce cell stiffness, and modulate Rho GTPase activities, cell tension's effects on the mechanosensory feedback during cytokinesis (reviewed in [156]) is intriguing. A previous study demonstrated that stem cell lineage commitment is also regulated by the factors of cell shape, cell tension and RhoA [157]. More relevantly, changes in cell volume and stiffness through hyperosmotic water efflux was recently observed to alter the differentiation pathway of mesenchymal stem cells [158]. It would be interesting to investigate to what extent osmotically driven cell tension modulation affects cell fate diversity in early *Xenopus* embryo

development [159]. In addition to reduced stiffness, sucrose-treated oocytes also performed more work, both of which are mechanical hallmarks of malignant cancer cells [160]. Indeed, patient tumor cell stiffness inversely correlates with their migration and invasion through 3D basement membranes [161]. Thus, cell tension's role in metastatic potential also has further investigative promise.

4.3.2. Other biological scales

Importantly, insights gained in studies of single-cell wound healing could also be applied to the multicellular level. Repair of epithelial tissues primarily involves the organized formation and contraction of a supracellular actomyosin ring which share structural and functional similarities to the actomyosin ring in oocyte wound healing (reviewed in [155, 162]). Specifically, RhoA-mediated coordination of actomyosin contraction via DIAPH and ROCK was observed to regulate Drosophila pupae epithelial repair [163] just as in *Xenopus* oocytes. Although it has since been suggested that just the actomyosin ring contraction is insufficient to explain the multidirectional force patterns during multicellular wound closure, the major force components of these patterns were still observed to arise from cell-derived tensions [164]. Also considering that the scarring region of skin wounds depends on natural skin tension [165, 166], modulating tension in these tissue models may lead to novel findings in biological scales larger than the single-cell level.

4.4. Future directions

4.4.1. CARhoA rescue of wound healing in sucrose-treated oocytes

Observation of exogenous rescue would definitively establish cell tension reduction-induced inhibition of RhoA's regulatory activity as the cause of disturbed actomyosin-mediated wound healing. This could be achieved by oocyte microinjection of a CARhoA probe with a RhoA point mutation at leucine 63 (pCS2-YFP-RhoA-L63) which renders its constitutive activity. It is expected that exogenous promotion of RhoA activity would at least partially rescue wound healing rates of sucrose-treated oocytes back to control levels (Figure 20).

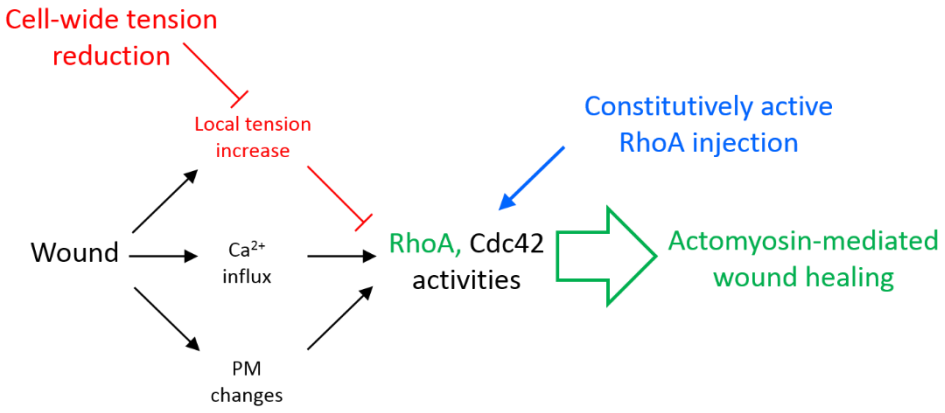

Figure 19. Experimental design: CARhoA-induced rescue of wound healing.

4.4.2. Further demonstrations of cell tension influence

Further demonstrations of RhoA and Cdc42 activities being influenced by cell tension should be performed to increase credibility of this study's hypothesis. Lysates of sucrose-treated oocytes which have been incubated back in control media could be analyzed. At least partial recovery of RhoA activity, and reversion of Cdc42 activity, back to control levels are expected. Additional

elastic microindentations with higher resolution methods could be performed to formulate a comprehensive stress-strain curve, which describes oocyte deformation across more compressive distances. Cell tension should also be mechanically modulated to reconcile the relative crudeness of sucrose media incubation. For example, oocytes could be cultured in a fibronectin coated polydimethylsiloxane (PDMS) membrane, which is molded and attached to an external stretch apparatus mounted on a confocal microscope, such that the oocyte is stretched and cell tension directly modulated prior to wounding (detailed in [167]). Another possible method applicable to mammalian cells would involve optical tweezers to stretch individual cells in a PDMS slide setup under the microscope (reviewed in [168, 169]).

4.4.3. Upstream mechanistic studies

Identifying upstream mechanisms of RhoA activity decrease and Cdc42 activity increase in sucrose-treated oocytes would shed more light on the mechanotransducive behaviors of Rho GTPases in response to mechanical wounds. The possible influences of cell tension reduction on local activity and localization of Rho GEF-GAP ABR could be investigated using established molecular probes [128]. Considering ABR's dual GEF-GAP functions of RhoA activation and Cdc42 inhibition (see Section 1.1.5.3), ABR activity being negatively affected by cell tension reduction would be consistent with downstream changes in RhoA, Cdc42 activities observed in sucrose-treated oocytes. The other Rho GEF-GAP BCR may also be affected by cell tension reduction and has yet to be directly investigated in the wound healing regulation context. Furthermore, since plasma membrane lipids contribute to Rho GTPase activity changes (see Section 1.1.5.2), wound-induced enrichment of lipids may also be affected. Specifically,

visualization of DAG activity and localization in oocytes could be compared with incorporation of its fluorescent reporter [125].

Chapter 5:
Conclusions

5. Conclusions

This study's hypothesis, that transient local tension increase is necessary for actomyosin-mediated wound healing, has been demonstrated. Cell tension reduction's negative influence on wound healing has been exhibited through perturbed closure, reduced actin enrichment, and inhibited local RhoA activity localization. These correlations explain actomyosin's mechanotransducive behavior in response to mechanical wounds. That said, cell tension's influence on actomyosin regulation by Rho GTPase activities has only begun to be uncovered. Upstream mechanisms of cell-wide RhoA inhibition and Cdc42 activation have yet to be determined. In addition to mechanistic studies, analogous experiments on mammalian cells which account for cell adhesive contributions, and definitive decoupling of cell tension through more mechanical methods should also be performed. Such future studies would comprehensively demonstrate cell tension's effects on actomyosin-mediated wound healing regulation. Nonetheless, this study has illustrated the cell's sensitivity to cell tension disequilibrium when responding to mechanical wounds.

VIII. Bibliography

1. Ingber, D.E., *Cellular tensegrity: defining new rules of biological design that govern the cytoskeleton.* J Cell Sci, 1993. **104 (Pt 3)**: p. 613-27.
2. Fuller, B. TENSILE-INTEGRITY STRUCTURES. USA. 3,063,521. Nov 13, 1962.
3. Barak, L.S., et al., *Fluorescence staining of the actin cytoskeleton in living cells with 7-nitrobenz-2-oxa-1,3-diazole-phallacidin.* Proc Natl Acad Sci U S A, 1980. **77**(2): p. 980-4.
4. Rafferty, N.S. and D.L. Scholz, *Actin in polygonal arrays of microfilaments and sequestered actin bundles (SABs) in lens epithelial cells of rabbits and mice.* Curr Eye Res, 1985. **4**(6): p. 713-8.
5. Entcheva, E. and H. Bien, *Mechanical and spatial determinants of cytoskeletal geodesic dome formation in cardiac fibroblasts.* Integr Biol (Camb), 2009. **1**(2): p. 212-9.
6. Wagenknecht, T., et al., *Cryoelectron microscopy of mammalian pyruvate dehydrogenase complex.* J Biol Chem, 1991. **266**(36): p. 24650-6.
7. Vigers, G.P., R.A. Crowther, and B.M. Pearse, *Three-dimensional structure of clathrin cages in ice.* EMBO J, 1986. **5**(3): p. 529-34.
8. Kasza, K.E., et al., *The cell as a material.* Curr Opin Cell Biol, 2007. **19**(1): p. 101-7.
9. Diz-Munoz, A., D.A. Fletcher, and O.D. Weiner, *Use the force: membrane tension as an organizer of cell shape and motility.* Trends Cell Biol, 2013. **23**(2): p. 47-53.
10. Stamenovic, D. and M.F. Coughlin, *The role of prestress and architecture of the cytoskeleton and deformability of cytoskeletal filaments in mechanics of adherent cells: a quantitative analysis.* J Theor Biol, 1999. **201**(1): p. 63-74.
11. Storm, C., et al., *Nonlinear elasticity in biological gels.* Nature, 2005. **435**(7039): p. 191-4.
12. Fernandez, P., P.A. Pullarkat, and A. Ott, *A master relation defines the nonlinear viscoelasticity of single fibroblasts.* Biophys J, 2006. **90**(10): p. 3796-805.
13. Gardel, M.L., et al., *Prestressed F-actin networks cross-linked by hinged filamins replicate mechanical properties of cells.* Proc Natl Acad Sci U S A, 2006. **103**(6): p. 1762-7.
14. Kang, J., et al., *Structurally governed cell mechanotransduction through multiscale modeling.* Sci Rep, 2015. **5**: p. 8622.
15. Ingber, D.E., N. Wang, and D. Stamenovic, *Tensegrity, cellular biophysics, and the mechanics of living systems.* Rep Prog Phys, 2014. **77**(4): p. 046603.
16. Kozlov, M.M. and L.V. Chernomordik, *Membrane tension and membrane fusion.* Curr Opin Struct Biol, 2015. **33**: p. 61-7.
17. Dai, J. and M.P. Sheetz, *Membrane tether formation from blebbing cells.* Biophys J, 1999. **77**(6): p. 3363-70.
18. Sheetz, M.P., *Cell control by membrane-cytoskeleton adhesion.* Nat Rev Mol Cell Biol, 2001. **2**(5): p. 392-6.
19. Bo, L. and R.E. Waugh, *Determination of bilayer membrane bending stiffness by tether formation from giant, thin-walled vesicles.* Biophys J, 1989. **55**(3): p. 509-17.
20. Waugh, R.E. and R.M. Hochmuth, *Mechanical equilibrium of thick, hollow, liquid membrane cylinders.* Biophys J, 1987. **52**(3): p. 391-400.
21. Evans, E.A. and R. Skalak, *Mechanics and thermodynamics of biomembranes: part 1.* CRC Crit Rev Bioeng, 1979. **3**(3): p. 181-330.

22. Evans, E.A., *Bending elastic modulus of red blood cell membrane derived from buckling instability in micropipet aspiration tests.* Biophys J, 1983. **43**(1): p. 27-30.
23. Fischer, T.M., *Bending stiffness of lipid bilayers. I. Bilayer couple or single-layer bending?* Biophys J, 1992. **63**(5): p. 1328-35.
24. Dimova, R., *Recent developments in the field of bending rigidity measurements on membranes.* Adv Colloid Interface Sci, 2014. **208**: p. 225-34.
25. Harbich, C., *[Compressive bandage of the lower limbs]*. Phlebologie, 1979. **32**(2): p. 159-63.
26. McNeil, P.L. and M.M. Baker, *Cell surface events during resealing visualized by scanning-electron microscopy.* Cell Tissue Res, 2001. **304**(1): p. 141-6.
27. Zhelev, V.S., et al., *[Significance of left ventricular structural changes in arterial hypertension for the prolongation of electric cardiac systole]*. Kardiologiia, 1992. **32**(5): p. 21-3.
28. Garcia-Saez, A.J., S. Chiantia, and P. Schwille, *Effect of line tension on the lateral organization of lipid membranes.* J Biol Chem, 2007. **282**(46): p. 33537-44.
29. Kuzmin, P.I., et al., *Line tension and interaction energies of membrane rafts calculated from lipid splay and tilt.* Biophys J, 2005. **88**(2): p. 1120-33.
30. Sheetz, M.P., J.E. Sable, and H.G. Dobereiner, *Continuous membrane-cytoskeleton adhesion requires continuous accommodation to lipid and cytoskeleton dynamics.* Annu Rev Biophys Biomol Struct, 2006. **35**: p. 417-34.
31. Grashoff, C., et al., *Measuring mechanical tension across vinculin reveals regulation of focal adhesion dynamics.* Nature, 2010. **466**(7303): p. 263-6.
32. Hochmuth, F.M., et al., *Deformation and flow of membrane into tethers extracted from neuronal growth cones.* Biophys J, 1996. **70**(1): p. 358-69.
33. Footer, M.J., et al., *Direct measurement of force generation by actin filament polymerization using an optical trap.* Proc Natl Acad Sci U S A, 2007. **104**(7): p. 2181-6.
34. Ehrlicher, A.J., et al., *Alpha-actinin binding kinetics modulate cellular dynamics and force generation.* Proc Natl Acad Sci U S A, 2015. **112**(21): p. 6619-24.
35. Nakamura, F., et al., *Structural basis of filamin A functions.* J Cell Biol, 2007. **179**(5): p. 1011-25.
36. Tsukita, S., S. Yonemura, and S. Tsukita, *ERM proteins: head-to-tail regulation of actin-plasma membrane interaction.* Trends Biochem Sci, 1997. **22**(2): p. 53-8.
37. Salbreux, G., G. Charras, and E. Paluch, *Actin cortex mechanics and cellular morphogenesis.* Trends Cell Biol, 2012. **22**(10): p. 536-45.
38. Kapus, A. and P. Janmey, *Plasma Membrane-Cortical Cytoskeleton Interactions: A Cell Biology Approach with Biophysical Considerations.* Comprehensive Physiology, 2013. **3**(3): p. 1231-1281.
39. Gittes, F., et al., *Flexural rigidity of microtubules and actin filaments measured from thermal fluctuations in shape.* J Cell Biol, 1993. **120**(4): p. 923-34.
40. Mohan, R. and A. John, *Microtubule-associated proteins as direct crosslinkers of actin filaments and microtubules.* IUBMB Life, 2015. **67**(6): p. 395-403.
41. Brangwynne, C.P., et al., *Microtubules can bear enhanced compressive loads in living cells because of lateral reinforcement.* J Cell Biol, 2006. **173**(5): p. 733-41.
42. Mendez, M.G., D. Restle, and P.A. Janmey, *Vimentin enhances cell elastic behavior and protects against compressive stress.* Biophys J, 2014. **107**(2): p. 314-323.

43. Chen, C., et al., *Effects of vimentin disruption on the mechanoresponses of articular chondrocyte.* Biochem Biophys Res Commun, 2016. **469**(1): p. 132-137.
44. Herrmann, H., et al., *Intermediate filaments: from cell architecture to nanomechanics.* Nat Rev Mol Cell Biol, 2007. **8**(7): p. 562-73.
45. Ingber, D.E., *Tensegrity I. Cell structure and hierarchical systems biology.* J Cell Sci, 2003. **116**(Pt 7): p. 1157-73.
46. Korn, E.D., M.F. Carlier, and D. Pantaloni, *Actin polymerization and ATP hydrolysis.* Science, 1987. **238**(4827): p. 638-44.
47. Weisenberg, R.C., G.G. Borisy, and E.W. Taylor, *The colchicine-binding protein of mammalian brain and its relation to microtubules.* Biochemistry, 1968. **7**(12): p. 4466-79.
48. Gaszner, B., et al., *Replacement of ATP with ADP affects the dynamic and conformational properties of actin monomer.* Biochemistry, 1999. **38**(39): p. 12885-92.
49. Horio, T. and T. Murata, *The role of dynamic instability in microtubule organization.* Front Plant Sci, 2014. **5**: p. 511.
50. Vavylonis, D., Q. Yang, and B. O'Shaughnessy, *Actin polymerization kinetics, cap structure, and fluctuations.* Proc Natl Acad Sci U S A, 2005. **102**(24): p. 8543-8.
51. Howard, J. and A.A. Hyman, *Dynamics and mechanics of the microtubule plus end.* Nature, 2003. **422**(6933): p. 753-8.
52. Cleveland, D.W., *Treadmilling of tubulin and actin.* Cell, 1982. **28**(4): p. 689-91.
53. Amann, K.J. and T.D. Pollard, *The Arp2/3 complex nucleates actin filament branches from the sides of pre-existing filaments.* Nat Cell Biol, 2001. **3**(3): p. 306-10.
54. Moritz, M., et al., *Structure of the gamma-tubulin ring complex: a template for microtubule nucleation.* Nat Cell Biol, 2000. **2**(6): p. 365-70.
55. Witke, W., *The role of profilin complexes in cell motility and other cellular processes.* Trends Cell Biol, 2004. **14**(8): p. 461-9.
56. Bamburg, J.R., *Proteins of the ADF/cofilin family: essential regulators of actin dynamics.* Annu Rev Cell Dev Biol, 1999. **15**: p. 185-230.
57. Kinoshita, K., B. Habermann, and A.A. Hyman, *XMAP215: a key component of the dynamic microtubule cytoskeleton.* Trends Cell Biol, 2002. **12**(6): p. 267-73.
58. Petry, S., et al., *Branching microtubule nucleation in Xenopus egg extracts mediated by augmin and TPX2.* Cell, 2013. **152**(4): p. 768-77.
59. Fletcher, D.A. and R.D. Mullins, *Cell mechanics and the cytoskeleton.* Nature, 2010. **463**(7280): p. 485-92.
60. Mandato, C.A. and W.M. Bement, *Actomyosin transports microtubules and microtubules control actomyosin recruitment during Xenopus oocyte wound healing.* Curr Biol, 2003. **13**(13): p. 1096-105.
61. Waterman-Storer, C.M. and E.D. Salmon, *Actomyosin-based retrograde flow of microtubules in the lamella of migrating epithelial cells influences microtubule dynamic instability and turnover and is associated with microtubule breakage and treadmilling.* J Cell Biol, 1997. **139**(2): p. 417-34.
62. Mandato, C.A., H.A. Benink, and W.M. Bement, *Microtubule-actomyosin interactions in cortical flow and cytokinesis.* Cell Motil Cytoskeleton, 2000. **45**(2): p. 87-92.
63. Andrews, N.W., P.E. Almeida, and M. Corrotte, *Damage control: cellular mechanisms of plasma membrane repair.* Trends Cell Biol, 2014. **24**(12): p. 734-42.

64. Boucher, E. and C.A. Mandato, *Plasma membrane and cytoskeleton dynamics during single-cell wound healing.* Biochim Biophys Acta, 2015. **1853**(10 Pt A): p. 2649-61.
65. Terasaki, M., K. Miyake, and P.L. McNeil, *Large plasma membrane disruptions are rapidly resealed by Ca2+-dependent vesicle-vesicle fusion events.* J Cell Biol, 1997. **139**(1): p. 63-74.
66. McNeil, P.L., et al., *Patching plasma membrane disruptions with cytoplasmic membrane.* J Cell Sci, 2000. **113 (Pt 11)**: p. 1891-902.
67. Freedman, J.C., et al., *Membrane potential and the cytotoxic Ca cascade of human red blood cells.* Soc Gen Physiol Ser, 1988. **43**: p. 217-31.
68. McNeil, P.L. and T. Kirchhausen, *An emergency response team for membrane repair.* Nat Rev Mol Cell Biol, 2005. **6**(6): p. 499-505.
69. Wang, L., et al., *Vacuole fusion at a ring of vertex docking sites leaves membrane fragments within the organelle.* Cell, 2002. **108**(3): p. 357-69.
70. Wang, L., et al., *Hierarchy of protein assembly at the vertex ring domain for yeast vacuole docking and fusion.* J Cell Biol, 2003. **160**(3): p. 365-74.
71. Davenport, N.R., et al., *Membrane dynamics during cellular wound repair.* Mol Biol Cell, 2016. **27**(14): p. 2272-85.
72. Abreu-Blanco, M.T., J.M. Verboon, and S.M. Parkhurst, *Cell wound repair in Drosophila occurs through three distinct phases of membrane and cytoskeletal remodeling.* J Cell Biol, 2011. **193**(3): p. 455-64.
73. Selman, G.G. and G.J. Pawsey, *The utilization of yolk platelets by tissues of Xenopus embryos studied by a safranin staining method.* J Embryol Exp Morphol, 1965. **14**(2): p. 191-212.
74. Reddy, A., E.V. Caler, and N.W. Andrews, *Plasma membrane repair is mediated by Ca(2+)-regulated exocytosis of lysosomes.* Cell, 2001. **106**(2): p. 157-69.
75. Jaiswal, J.K., N.W. Andrews, and S.M. Simon, *Membrane proximal lysosomes are the major vesicles responsible for calcium-dependent exocytosis in nonsecretory cells.* J Cell Biol, 2002. **159**(4): p. 625-35.
76. Andrews, N.W., P.E. Almeida, and M. Corrotte, *Damage control: cellular mechanisms of plasma membrane repair.* Trends Cell Biol, 2014. **24**(12): p. 734-742.
77. Mandato, C.A. and W.M. Bement, *Contraction and polymerization cooperate to assemble and close actomyosin rings around Xenopus oocyte wounds.* J Cell Biol, 2001. **154**(4): p. 785-97.
78. Bement, W.M., C.A. Mandato, and M.N. Kirsch, *Wound-induced assembly and closure of an actomyosin purse string in Xenopus oocytes.* Curr Biol, 1999. **9**(11): p. 579-87.
79. Benink, H.A. and W.M. Bement, *Concentric zones of active RhoA and Cdc42 around single cell wounds.* J Cell Biol, 2005. **168**(3): p. 429-39.
80. Kimura, K., et al., *Regulation of myosin phosphatase by Rho and Rho-associated kinase (Rho-kinase).* Science, 1996. **273**(5272): p. 245-8.
81. Kawano, Y., et al., *Phosphorylation of myosin-binding subunit (MBS) of myosin phosphatase by Rho-kinase in vivo.* J Cell Biol, 1999. **147**(5): p. 1023-38.
82. Watanabe, N., et al., *p140mDia, a mammalian homolog of Drosophila diaphanous, is a target protein for Rho small GTPase and is a ligand for profilin.* EMBO J, 1997. **16**(11): p. 3044-56.
83. Watanabe, N., et al., *Cooperation between mDia1 and ROCK in Rho-induced actin reorganization.* Nat Cell Biol, 1999. **1**(3): p. 136-43.

84. Nakano, K., et al., *Distinct actions and cooperative roles of ROCK and mDia in Rho small G protein-induced reorganization of the actin cytoskeleton in Madin-Darby canine kidney cells.* Mol Biol Cell, 1999. **10**(8): p. 2481-91.
85. Rohatgi, R., et al., *The interaction between N-WASP and the Arp2/3 complex links Cdc42-dependent signals to actin assembly.* Cell, 1999. **97**(2): p. 221-31.
86. Egile, C., et al., *Activation of the CDC42 effector N-WASP by the Shigella flexneri IcsA protein promotes actin nucleation by Arp2/3 complex and bacterial actin-based motility.* J Cell Biol, 1999. **146**(6): p. 1319-32.
87. Cox, A.D. and C.J. Der, *Ras history: The saga continues.* Small GTPases, 2010. **1**(1): p. 2-27.
88. Goitre, L., et al., *The Ras superfamily of small GTPases: the unlocked secrets.* Methods Mol Biol, 2014. **1120**: p. 1-18.
89. Aspenstrom, P., A. Fransson, and J. Saras, *Rho GTPases have diverse effects on the organization of the actin filament system.* Biochem J, 2004. **377**(Pt 2): p. 327-37.
90. Paterson, H.F., et al., *Microinjection of recombinant p21rho induces rapid changes in cell morphology.* J Cell Biol, 1990. **111**(3): p. 1001-7.
91. Jaffe, A.B. and A. Hall, *Rho GTPases: biochemistry and biology.* Annu Rev Cell Dev Biol, 2005. **21**: p. 247-69.
92. Cherfils, J. and M. Zeghouf, *Regulation of small GTPases by GEFs, GAPs, and GDIs.* Physiol Rev, 2013. **93**(1): p. 269-309.
93. Hodge, R.G. and A.J. Ridley, *Regulating Rho GTPases and their regulators.* Nat Rev Mol Cell Biol, 2016. **17**(8): p. 496-510.
94. Lang, P., et al., *Protein kinase A phosphorylation of RhoA mediates the morphological and functional effects of cyclic AMP in cytotoxic lymphocytes.* EMBO J, 1996. **15**(3): p. 510-9.
95. Ellerbroek, S.M., K. Wennerberg, and K. Burridge, *Serine phosphorylation negatively regulates RhoA in vivo.* J Biol Chem, 2003. **278**(21): p. 19023-31.
96. Bishop, A.L. and A. Hall, *Rho GTPases and their effector proteins.* Biochem J, 2000. **348 Pt 2**: p. 241-55.
97. Maekawa, M., et al., *Signaling from Rho to the actin cytoskeleton through protein kinases ROCK and LIM-kinase.* Science, 1999. **285**(5429): p. 895-8.
98. Madaule, P., et al., *Role of citron kinase as a target of the small GTPase Rho in cytokinesis.* Nature, 1998. **394**(6692): p. 491-4.
99. Teramoto, H., et al., *The small GTP-binding protein rho activates c-Jun N-terminal kinases/stress-activated protein kinases in human kidney 293T cells. Evidence for a Pak-independent signaling pathway.* J Biol Chem, 1996. **271**(42): p. 25731-4.
100. Fanger, G.R., N.L. Johnson, and G.L. Johnson, *MEK kinases are regulated by EGF and selectively interact with Rac/Cdc42.* EMBO J, 1997. **16**(16): p. 4961-72.
101. Chou, M.M. and J. Blenis, *The 70 kDa S6 kinase complexes with and is activated by the Rho family G proteins Cdc42 and Rac1.* Cell, 1996. **85**(4): p. 573-83.
102. Gilmore, A.P. and K. Burridge, *Regulation of vinculin binding to talin and actin by phosphatidyl-inositol-4-5-bisphosphate.* Nature, 1996. **381**(6582): p. 531-5.
103. Ren, X.D., et al., *Physical association of the small GTPase Rho with a 68-kDa phosphatidylinositol 4-phosphate 5-kinase in Swiss 3T3 cells.* Mol Biol Cell, 1996. **7**(3): p. 435-42.

104. Tolias, K.F., L.C. Cantley, and C.L. Carpenter, *Rho family GTPases bind to phosphoinositide kinases.* J Biol Chem, 1995. **270**(30): p. 17656-9.
105. Han, J.S., et al., *The potential role for CDC42 protein from rat brain cytosol in phospholipase D activation.* Biochem Mol Biol Int, 1998. **45**(6): p. 1089-103.
106. Bae, C.D., et al., *Determination of interaction sites on the small G protein RhoA for phospholipase D.* J Biol Chem, 1998. **273**(19): p. 11596-604.
107. Burkel, B.M., et al., *A Rho GTPase signal treadmill backs a contractile array.* Dev Cell, 2012. **23**(2): p. 384-96.
108. Bement, W.M., et al., *Activator-inhibitor coupling between Rho signalling and actin assembly makes the cell cortex an excitable medium.* Nat Cell Biol, 2015. **17**(11): p. 1471-83.
109. Li, Z., C.D. Aizenman, and H.T. Cline, *Regulation of rho GTPases by crosstalk and neuronal activity in vivo.* Neuron, 2002. **33**(5): p. 741-50.
110. Matsukawa, T., et al., *Mechanisms of RhoA inactivation and CDC42 and Rac1 activation during zebrafish optic nerve regeneration.* Neurochem Int, 2018. **112**: p. 71-80.
111. Martin, E., M.H. Ouellette, and S. Jenna, *Rac1/RhoA antagonism defines cell-to-cell heterogeneity during epidermal morphogenesis in nematodes.* J Cell Biol, 2016. **215**(4): p. 483-498.
112. Kim, S.Y., et al., *Coordinated balance of Rac1 and RhoA plays key roles in determining phagocytic appetite.* PLoS One, 2017. **12**(4): p. e0174603.
113. Berridge, M.J., P. Lipp, and M.D. Bootman, *The versatility and universality of calcium signalling.* Nat Rev Mol Cell Biol, 2000. **1**(1): p. 11-21.
114. O'Brien, E.T., E.D. Salmon, and H.P. Erickson, *How calcium causes microtubule depolymerization.* Cell Motil Cytoskeleton, 1997. **36**(2): p. 125-35.
115. Togo, T., *Disruption of the plasma membrane stimulates rearrangement of microtubules and lipid traffic toward the wound site.* J Cell Sci, 2006. **119**(Pt 13): p. 2780-6.
116. Narita, A., et al., *Ca(2+)-induced switching of troponin and tropomyosin on actin filaments as revealed by electron cryo-microscopy.* J Mol Biol, 2001. **308**(2): p. 241-61.
117. Wakabayashi, T., *Mechanism of the calcium-regulation of muscle contraction--in pursuit of its structural basis.* Proc Jpn Acad Ser B Phys Biol Sci, 2015. **91**(7): p. 321-50.
118. Huang, K.P., *The mechanism of protein kinase C activation.* Trends Neurosci, 1989. **12**(11): p. 425-32.
119. Barandier, C., et al., *PKC is required for activation of ROCK by RhoA in human endothelial cells.* Biochem Biophys Res Commun, 2003. **304**(4): p. 714-9.
120. McNeil, P.L., K. Miyake, and S.S. Vogel, *The endomembrane requirement for cell surface repair.* Proc Natl Acad Sci U S A, 2003. **100**(8): p. 4592-7.
121. Bansal, D., et al., *Defective membrane repair in dysferlin-deficient muscular dystrophy.* Nature, 2003. **423**(6936): p. 168-72.
122. Mellgren, R.L., et al., *Calpain is required for the rapid, calcium-dependent repair of wounded plasma membrane.* J Biol Chem, 2007. **282**(4): p. 2567-75.
123. Lu, P.J., et al., *Lipid products of phosphoinositide 3-kinase bind human profilin with high affinity.* Biochemistry, 1996. **35**(44): p. 14027-34.
124. Faure, J., P.V. Vignais, and M.C. Dagher, *Phosphoinositide-dependent activation of Rho A involves partial opening of the RhoA/Rho-GDI complex.* Eur J Biochem, 1999. **262**(3): p. 879-89.

125. Vaughan, E.M., et al., *Lipid domain-dependent regulation of single-cell wound repair.* Mol Biol Cell, 2014. **25**(12): p. 1867-76.
126. Yu, H.Y. and W.M. Bement, *Control of local actin assembly by membrane fusion-dependent compartment mixing.* Nat Cell Biol, 2007. **9**(2): p. 149-59.
127. Holmes, W.R., et al., *Modeling the roles of protein kinase Cbeta and eta in single-cell wound repair.* Mol Biol Cell, 2015. **26**(22): p. 4100-8.
128. Vaughan, E.M., et al., *Control of local Rho GTPase crosstalk by Abr.* Curr Biol, 2011. **21**(4): p. 270-7.
129. Simon, C.M., et al., *Pattern formation of Rho GTPases in single cell wound healing.* Mol Biol Cell, 2013. **24**(3): p. 421-32.
130. Holmes, W.R., et al., *A mathematical model of GTPase pattern formation during single-cell wound repair.* Interface Focus, 2016. **6**(5): p. 20160032.
131. Cho, Y.J., et al., *Abr and Bcr, two homologous Rac GTPase-activating proteins, control multiple cellular functions of murine macrophages.* Mol Cell Biol, 2007. **27**(3): p. 899-911.
132. McNeil, P.L. and M. Terasaki, *Coping with the inevitable: how cells repair a torn surface membrane.* Nat Cell Biol, 2001. **3**(5): p. E124-9.
133. Meldolesi, J., *Surface wound healing: a new, general function of eukaryotic cells.* J Cell Mol Med, 2003. **7**(3): p. 197-203.
134. Schweitzer, Y., et al., *Theoretical analysis of membrane tension in moving cells.* Biophys J, 2014. **106**(1): p. 84-92.
135. Diz-Munoz, A., et al., *Membrane Tension Acts Through PLD2 and mTORC2 to Limit Actin Network Assembly During Neutrophil Migration.* PLoS Biol, 2016. **14**(6): p. e1002474.
136. Gauthier, N.C., et al., *Temporary increase in plasma membrane tension coordinates the activation of exocytosis and contraction during cell spreading.* Proc Natl Acad Sci U S A, 2011. **108**(35): p. 14467-72.
137. Masters, T.A., et al., *Plasma membrane tension orchestrates membrane trafficking, cytoskeletal remodeling, and biochemical signaling during phagocytosis.* Proc Natl Acad Sci U S A, 2013. **110**(29): p. 11875-80.
138. Iskratsch, T., H. Wolfenson, and M.P. Sheetz, *Appreciating force and shape-the rise of mechanotransduction in cell biology.* Nat Rev Mol Cell Biol, 2014. **15**(12): p. 825-33.
139. Di Ciano, C., et al., *Osmotic stress-induced remodeling of the cortical cytoskeleton.* Am J Physiol Cell Physiol, 2002. **283**(3): p. C850-65.
140. Di Ciano-Oliveira, C., et al., *Hyperosmotic stress activates Rho: differential involvement in Rho kinase-dependent MLC phosphorylation and NKCC activation.* Am J Physiol Cell Physiol, 2003. **285**(3): p. C555-66.
141. Moeendarbary, E. and A.R. Harris, *Cell mechanics: principles, practices, and prospects.* Wiley Interdiscip Rev Syst Biol Med, 2014. **6**(5): p. 371-88.
142. Liu, X., et al., *Elastic and viscoelastic characterization of mouse oocytes using micropipette indentation.* Ann Biomed Eng, 2012. **40**(10): p. 2122-30.
143. Terry, S.J., et al., *Spatially restricted activation of RhoA signalling at epithelial junctions by p114RhoGEF drives junction formation and morphogenesis.* Nat Cell Biol, 2011. **13**(2): p. 159-66.
144. Reyes, C.C., et al., *Anillin regulates cell-cell junction integrity by organizing junctional accumulation of Rho-GTP and actomyosin.* Curr Biol, 2014. **24**(11): p. 1263-70.

145. Burg, M.B., J.D. Ferraris, and N.I. Dmitrieva, *Cellular response to hyperosmotic stresses.* Physiol Rev, 2007. **87**(4): p. 1441-74.
146. Michea, L., et al., *Mitochondrial dysfunction is an early event in high-NaCl-induced apoptosis of mIMCD3 cells.* Am J Physiol Renal Physiol, 2002. **282**(6): p. F981-90.
147. Horn, A., et al., *Mitochondrial redox signaling enables repair of injured skeletal muscle cells.* Sci Signal, 2017. **10**(495).
148. Khalilian, M., et al., *Estimating Young's modulus of zona pellucida by micropipette aspiration in combination with theoretical models of ovum.* J R Soc Interface, 2010. **7**(45): p. 687-94.
149. Kelly, S.M., Y.L. Jia, and P.T. Macklem, *Measurement of elastic properties of Xenopus oocytes.* Comp Biochem Physiol A Physiol, 1997. **118**(3): p. 607-13.
150. Yonemura, S., K. Hirao-Minakuchi, and Y. Nishimura, *Rho localization in cells and tissues.* Exp Cell Res, 2004. **295**(2): p. 300-14.
151. Stephenson, R.E. and A.L. Miller, *Tools for live imaging of active Rho GTPases in Xenopus.* Genesis, 2017. **55**(1-2).
152. Soto, X., et al., *Inositol kinase and its product accelerate wound healing by modulating calcium levels, Rho GTPases, and F-actin assembly.* Proc Natl Acad Sci U S A, 2013. **110**(27): p. 11029-34.
153. Darenfed, H. and C.A. Mandato, *Wound-induced contractile ring: a model for cytokinesis.* Biochem Cell Biol, 2005. **83**(6): p. 711-20.
154. Bement, W.M. and G. von Dassow, *Single cell pattern formation and transient cytoskeletal arrays.* Curr Opin Cell Biol, 2014. **26**: p. 51-9.
155. Schwayer, C., et al., *Actin Rings of Power.* Dev Cell, 2016. **37**(6): p. 493-506.
156. Mohan, K., P.A. Iglesias, and D.N. Robinson, *Separation anxiety: stress, tension and cytokinesis.* Exp Cell Res, 2012. **318**(12): p. 1428-34.
157. McBeath, R., et al., *Cell shape, cytoskeletal tension, and RhoA regulate stem cell lineage commitment.* Dev Cell, 2004. **6**(4): p. 483-95.
158. Guo, M., et al., *Cell volume change through water efflux impacts cell stiffness and stem cell fate.* Proc Natl Acad Sci U S A, 2017. **114**(41): p. E8618-E8627.
159. Chalmers, A.D., B. Strauss, and N. Papalopulu, *Oriented cell divisions asymmetrically segregate aPKC and generate cell fate diversity in the early Xenopus embryo.* Development, 2003. **130**(12): p. 2657-68.
160. Guo, M., et al., *Probing the stochastic, motor-driven properties of the cytoplasm using force spectrum microscopy.* Cell, 2014. **158**(4): p. 822-832.
161. Swaminathan, V., et al., *Mechanical stiffness grades metastatic potential in patient tumor cells and in cancer cell lines.* Cancer Res, 2011. **71**(15): p. 5075-80.
162. Sonnemann, K.J. and W.M. Bement, *Wound repair: toward understanding and integration of single-cell and multicellular wound responses.* Annu Rev Cell Dev Biol, 2011. **27**: p. 237-63.
163. Antunes, M., et al., *Coordinated waves of actomyosin flow and apical cell constriction immediately after wounding.* J Cell Biol, 2013. **202**(2): p. 365-79.
164. Brugues, A., et al., *Forces driving epithelial wound healing.* Nat Phys, 2014. **10**(9): p. 683-690.
165. Burgess, L.P., et al., *Wound healing. Relationship of wound closing tension to scar width in rats.* Arch Otolaryngol Head Neck Surg, 1990. **116**(7): p. 798-802.
166. Cerda, E., *Mechanics of scars.* J Biomech, 2005. **38**(8): p. 1598-603.

167. Stooke-Vaughan, G.A., L.A. Davidson, and S. Woolner, *Xenopus as a model for studies in mechanical stress and cell division.* Genesis, 2017. **55**(1-2).
168. Zhang, H. and K.K. Liu, *Optical tweezers for single cells.* J R Soc Interface, 2008. **5**(24): p. 671-90.
169. Yang, T., F. Bragheri, and P. Minzioni, *A Comprehensive Review of Optical Stretcher for Cell Mechanical Characterization at Single-Cell Level.* Micromachines, 2016. **7**(5).